UNIVERSITY OF MISKOLC
FACULTY OF MECHANICAL ENGINEERING AND INFORMATICS

DESIGN, DEVELOPMENT, AND OPTIMIZATION OF SOLAR DRYER FOR WOOD FUELS

Booklet of PhD Thesis

PREPARED BY:

BAIBHAW KUMAR

Mechanical Engineering (BE),
Energy Technology-Mechanical (M-Tech)

ISTVÁN SÁLYI DOCTORAL SCHOOL OF MECHANICAL ENGINEERING SCIENCES
TOPIC FIELD OF DESIGN OF MACHINES AND STRUCTURES
TOPIC GROUP OF ENERGY AND CHEMICAL ENGINEERING SYSTEMS DESIGN

Head of Doctoral School

Prof. Dr. Gabriella Bognár
DSc, Full Professor

Head of Topic Group

Prof. Dr. Zoltán Siménfalvi

Scientific Supervisor
Dr. Zoltán Szamosi

Scientific Co-Supervisor
Prof. Dr. Gábor L. Szepesi

Miskolc
2024

Table of Contents

LIST OF SYMBOLS AND ABBREVIATIONS

Q_I	absorbed energy (W)	n	lifespan (years)
Q_u	useful energy (W)	R	universal gas constant (8.314 J/mol.K)
Q_{st}	stored energy (W)	$\frac{W_{Tch}}{T_{ch}}$	temperature uncertainty
Q_l	lost energy (W)	$\frac{W_{\dot{m}a}}{\dot{m}a}$	mass-flow rate uncertainty
ρ	density (kg/m^3)	$\frac{W_{Eout}}{E_{out}}$	energy uncertainty
V_{avg}	average velocity (m/s)	N	payback period (years)
β	tilt angle [°]	ϕ	latitute angle (degree°)
A_{duct}	duct area (m^2)	f	inflation rate (%)
V_o	volume outside (m^3)	W_o	absolute humidity outside
V_i	volume inside (m^3)	W_i	absolute humidity inside
c	specific heat of sawdust (J/kg/K)	***Abbreviations***	
T_o	outlet temperature (°C)	PCM	phase change material
T_i	inlet temperature (°C)	PV	photovoltaics
A_c	collector area (m^2)	TES	thermal energy storage
I_T	radiation flux density (W/m^2)	DSC	differential scanning calorimetry
Q_{ch}	energy while charging (W)	CRF	capital recovery factor
Q_{dis}	energy while discharging (W)	FAC	fixed annual cost
$\dot{m}$	mass flowrate (kg/s)	SFF	sinking fund factor
ΔT	temperature difference	ASV	annual salvage value
η_{th}	thermal energy efficiency (%)	AMC	annual operational cost
T_a	ambient temperature (°C)	FAC	fixed annual cost
Ex_{in}	inlet exergy (W)	EBPT	energy payback time
Ex_u	outlet exergy (W)	IP	improvement potential
i	interest rate (%)	LOP	lack of productivity
η_{ex}	exergy efficiency	IC	capital cost of dryer
L	latent heat, J/kg	EUR	euros

1. INTRODUCTION

In the context of drying, the solar drying technique for maintaining wood fuel quality is common in many countries with reasonable solar radiation through solar kilns. The solar kiln designing and prototyping started more after the energy crisis of 1970. Lianbai [1]extensively investigated wood drying techniques in China a decade ago. The review suggests that the Chinese kilns for hardwood drying are slower and emphasize larger thermal capacity and a higher rate of air circulation. The effectiveness of solar drying depends not only on input temperature but several factors of the designed solar kiln. The solar insolation varies, and so does the wood moisture content and the atmosphere's humidity. The epochal weather conditions limit the drying rate; thus, heat storage mediums are important in drying technology innovations. Pushpendra et al. [2], identified such limitations in their review. The study suggested using PV/T and thermal energy storage mediums to improve the dryer efficiency. Research conducted by Dundar et al. [3]predicts that the requirement for woody biomass demand will rise soon. However, the study on solar drying or wood as biomass and its quality improvement through solar drying is covered to a small extent.

Researchers reviewed the vacuum-drying of wood by categorizing them into four groups: conductive heating vacuum, cyclic vacuum, superheated steam vacuum, and dielectric vacuum. Review work is also available on solar drying techniques, emphasizing types, parameters, and limitations with context on the economic and environmental assessment of various solar dryers . Yi *et al.* [4] presented the progress by reviewing cutting-edge drying technologies, including solar drying, microwave drying, and far-infrared drying at the laboratory and pilot-plant scale for biomass drying. In a recent review work by Lmarani et al. [5], the authors identified that the number of publications related to solar wood drying increased in the last five years. However, very limited review articles have been published. Also, they added that the solar drying of "wood" is a complex phenomenon depending on several factors. Therefore, further reviews and research can provide additional insights focusing on solar wood drying. Through this research, the intention is to bridge the gap and, at the same time, provide factual information linking solar energy utilization and the need for improving the fuel quality of wood for its use in process industries. The intrinsic pathways and methodologies researchers worldwide adopted in solar drying of different wood forms are addressed and discussed in detail. In addition, the thesis also explores the solar potential of Hungary through a trendline data assessment of the last ten years. The prime objectives of the research work carried out in this dissertation are as follows:

- To explore and review the classification of solar wood dryers and the various modeling approaches prevalent in the optimization of the drying system performances. In addition, An intrinsic global mapping of wood as biofuel production and review work of the solar drying systems used in various parts of the

world can provide insights into the type of wood being stored and dried with distinctive methods.

- To construct and the plot the temperature profile for a box-type natural convection solar dryer for drying of wood-chips.
- To develop a forced convection cabinet-type solar dryer and investigate the energy efficiency of the dryer for the three most commonly used wood fuels, i.e., woodchips, sawdust, and pellets.
- To develop a validation model using an artificial neural network (ANN) on MATLAB for the prediction of moisture content during the solar drying process.
- To demarcate the optimization of the solar dryer with and without phase change material (coconut oil) in terms of exergetic and energetic thermal performance.
- To evaluate the economic and environmental impact of hybrid solar drying of wood fuels.
- To identify the solar potential of the Hungarian region and investigate the problems in the quality of wood fuels at the boiler plant operations in Miskolc, Hungary, through trendline analysis of data.
- To propose and suggest potential reforms for the long-term storage and maintenance of the quality of wood fuels in largescale utilities.

2. MATERIALS AND METHODOLOGY

2.1.Methodology for Natural Convection Solar Dryer

Open-air solar drying is frequently regarded as the simplest and least expensive drying method. This technique has been around for a while in the area of agriculture and crop production. The main problem with open sun drying is the unpredictable drying rates, and dehydrating takes the most extended amount of time. The final quality is also impacted by uneven heating and varying drying rates. Depending on the customer's precise needs, solar dryers of various designs can manage these unfavorable aspects of open drying. The primary construction factors for a solar drier are the physical parameters, such as drying rate, temperature control, heat ventilation, etc. In this study, a direct-type natural convective lab-scale dryer was designed and developed to understand temperature profiling during different winter seasons. The dryer's sir flow is passive in nature and does not require any external fan or blower. The temperature inside the dryer rises during the afternoon and slowly declines with the sunset. This temperature rise gradually increases the dehydration of the product inside the cabinet. The drying efficiency differs for various products and needs different optimal moisture content. Dryers could also be designed based on the size of the agricultural product that needs to be dried. Forced dryers are commonly used in cases where a high heat requirement is required for the faster drying process. The airflow increases the heat transfer inside the chamber, directly affecting the drying rate. The cabinet dryer is mainly used to dry small items such as spices, grapes, banana chips, potatoes, chilly flakes, wood chips, etc. In most cases, it was observed that the drying rate was mainly 2 to 5 times faster than in open sun during models in agricultural products.

The lab-scale cabinet dryer was developed at the institute laboratory of the University of Miskolc. Figure. 1 (a) below depicts the 3D view of the dryer (all mentioned dimensions are in millimeters) and Figure. 1 (b) shows the real-time arrangement of the experiment with the dryer having the woodchips inside. The dryer's upper part is a transparent glass cover to maximize the heat trap inside the dryer. The inlet and outlet ventilation was provided on the two sides. These ventilation outlets were used to measure the temperature variation inside the dryer. The experiment intended to trap the sensible heat inside and its behavior during the experimental hours of the respective days.

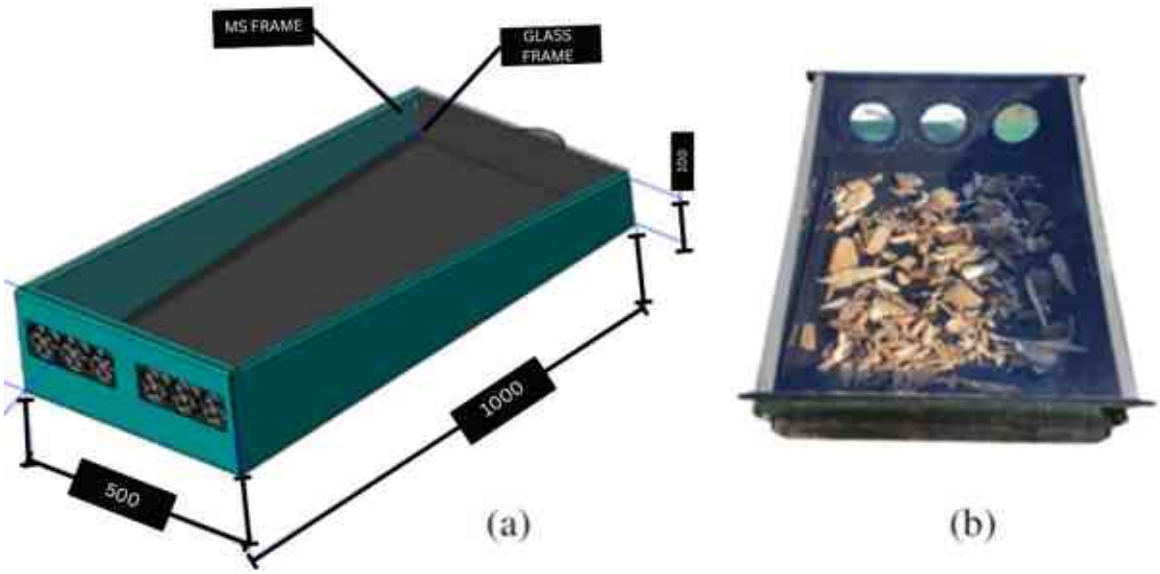

Figure 1. (a) 3D view of the dryer (all mentioned dimensions are in millimeters) (b) realtime arrangement of the experiment with the dryer having the woodchips inside.

2.2.Methodology for Forced Convection Solar Dryer

A forced convective cabinet solar dryer was prepared for this study at the University of Miskolc, Hungary. The dryer's body is made of wooden blocks, which are 2.5 cm thick and well-insulated on all sides. The size of the drying chamber (Length x Breadth x Height) is (80x50x45) cm. Thus, the total capacity of the dryer is 180,000 cm^3, i.e. 180 liters by volume. The drying cabinet consists of three trays separated by a distance of 7.5 cm. However, the pressure drop across the height was not considered while designing the drying system. On the top of the cabinet, a 50 cm long chimney is placed for the throughput of outlet air. The hot air solar collector attached to the dryer has an inclination of 40°. Transparent glass material is used for the air collector. For the air collector to provide ample air circulation and heat transfer, the length of the collector should be higher than its width [6]. Literature suggests the aspect ratio (Length: Width) be around 2 [7]. Based on (Length x Width), i.e. (40 x 60) cms, the aspect ratio of the proposed collector is 1.5. However, it can be improved further with size modification.The latitude angle (ϕ) of the location where drying is to be done is generally very closely related to the angle of inclination of the collector (β) or the tilt angle, given that the collector's face must be facing south-north [7]. In general, the inclination angle is given as [8]:

$$\beta = \phi + 10^0 \qquad (1)$$

Based on the coordinates of the city of Miskolc, i.e., 48°06′15″N 20°47′30″, the inclination angle was kept at 40° due to glass material size constraint. However, it can be improved further to around 60°.

Six inlet holes are provided for the air inlet with a diameter of 2 cm and three outlet holes with a diameter of 6 cm, which are joined to the drying cabinet. All sides of the dryer are painted black for the maximum heat trap inside the cabinet. The dryer's back view shows that the three trays consist of three different drying products. The bottom trays consist of woodchips, the middle one sawdust, and the top tray consists of the pellets. Table 1. depicts the design considerations considered in the experimental setup. These parameters are crucial for getting clear insights into the experiments and the various materials involved in the study.

Table 1. Design items and descriptions considered during the experiments.

Item	Details	Units
Drying Products	Woodchips, Sawdust, Pellets	-
Weight of Product	1	kg/pcs
Duration of Experiment/day	10 A.M. – 3 P.M.	h
Thickness of walls	2.5	cm
Thickness of collector glass	5	mm
Transmissivity of glass	0.89	Approx value
Number of trays	3	-
Capacity of Dryer	180	l
Type of air flow	Forced Convection	AC power supply
Load capacity	6	kg
Drying time	5	h

The experiments were carried out in the first and second week of October 2022 and best irradiation results were considered for calculations. The whole body of the dryer and the collector is made of wooden blocks, and sealant was used to fill the gaps to avoid heat loss from the system. The body was coated with black paint to enhance heat absorptivity. Experiments were conducted during the prime sunshine hours of the day, i.e., 10 A.M. to 3 P.M. The highest Radiation mainly was recorded between 12-1 P.M. Henceforth; the temperature rise inside the collector and dryer was also maximum during these hours. The anemometer measured the air inlet speed, which was controlled by the fan's speed at the top of the chimney. For all experiments, the air inlet speed was maintained at 2 m/s. An AC-powered fan was used at the top chimney to maintain this air flow rate. A multichannel data logger measured the temperature at six different locations of the inlet and outlets of the system. The relative humidity was measured using an (RH) meter valid in the range of 10-90 %. The sample's initial and end weights and moisture content were measured on the weight and moisture balances. All these apparatuses were utilized to take measurements as per the required parameters described in the methodology section.

The performance of the solar dryer is determined by the energy and exergy efficiency of the system. The efficiency of the dryer is coherent with the thermal efficiency of the solar air collector attached to the dryer. The temperature difference at the inlet T_i (°C) and outlet T_o (°C) of the collectors is used to calculate the useful heat energy Q_u of the collector, which is represented in Equation 2. C_p is the specific heat capacity of air at known temperature (J/(kg·K)) and ($\dot{m}$)be the mass flow rate of air at a given temperature (kg/s) [9].

$$Q_u = \dot{m} C_p (T_o - T_i) \tag{2}$$

The mass flow rate can be calculated as the product of the air density ρ (kg/m^3), average air velocity V (m/s) at the inlet of the collector, and the cross-section area $A_{collector}$ (m^2) of the duct [9] [10].

$$\dot{m} = \rho V A_{collector} \tag{3}$$

The amount of solar radiation absorbed by the collector is the amount of heat input to the system. The heat input Q_I is the product of solar Radiation I_T (W/m^2) falling on the collector and the surface area A_c (m^2) on which the radiation is falling [11]. Considering the transmissivity (τ) of the glass cover as 0.89 and assumed efficiency (η) of 0.9. Q_I is the proportion of total incident radiation received (I_T) on the air collector [7].

$$Q_I = I_T A_c \tag{4}$$

The ratio of useful heat in the system to the input heat energy falling on the collector gives the thermal efficiency for the solar air collector. The thermal efficiency of the collector influences the temperature inside the drying chamber directly. The drying rate of the wood fuel enhances with better efficiency [11].

$$\eta_{th,c} = \frac{\dot{m} C_p (T_o - T_i)}{I_T A_c} \tag{5}$$

The concept of exergy gain is based on the second law of thermodynamics. Thermal systems constitute available and unavailable energy parts known as "exergy" and "anergy" respectively. Exergy efficiency is defined as the proportion of energy or exergy in the fuel utilized to make the product. Exergy analysis's primary goal is to calculate the exergy destruction in various thermal system components [12]. The exergy gain can be defined as the rise in exergy during the airflows inside the collector. Equation (7) gives the exergy increase where, $\frac{\rho_o}{\rho_i}$ is the ratio of air density at outlet and inlet, and R is the air gap Rayleigh number [13]. The inlet exergy depends on solar radiation and the absorbing surfaces [11]. The T_s temperature of solar intensity was considered as 5600 K, whereas T_a is the ambient temperature in Kelvin as the

C_v is in (J/kg·K) . The ratio of the increase in exergy outlet and the inlet gives the exergy efficiency. The dryer performs better with better exergy efficiency [11] [14].

$$Ex_u = \dot{m}\left[C_p(T_o - T_i) - T_a\left(C_v \ln\left(\frac{T_o}{T_i}\right) - R\ln\left(\frac{\rho_o}{\rho_i}\right)\right)\right] \tag{6}$$

$$Ex_{in} = \left[1 + \frac{1}{3}\left(\frac{T_a}{T_s}\right)^4 - \frac{4}{3}\frac{T_a}{T_s}\right] I_T A_c \tag{7}$$

$$\eta_{th} = \frac{Ex_u}{Ex_{in}} \tag{8}$$

The type of material, the level of bound and unbound moisture, whether they are hygroscopic or non-hygroscopic, and the physical characteristics of the air utilized all impact how much moisture can be removed and then how efficiently. Non-hygroscopic materials can be dried to a moisture level of zero whereas hygroscopic materials will always have some residual moisture. The Moisture content (MC) helps plot the process's drying curve. The drying curve could be plotted MC (Wet/Dry) v/s Time, drying rate v/s MC or drying rate v/s time. In the experiments, MC was calculated on moisture (wet basis) using the moisture balance as the initial M_i and final M_f values pre and post-experiment [15]. Also, the moisture ratio MR is calculated as the ratio of M_t (moisture content at any time) v/s M_o (moisture content initial) [16].

$$MC = \frac{(M_i - M_f)}{M_i} \cdot 100 \tag{9}$$

$$MR = \frac{M_t}{M_o} \tag{10}$$

The amount of moisture removed m_{water} (kg) can be calculated considering the mass of the product to be dried (m_i) (kg) and the heat required to evaporate the water is given as Q (kJ). $m_{water}h_{fg}$ represents consumed energy to evaporate water from the drying product [11]. The overall drying efficiency of the system is a ratio as shown in equation (14) where there are additional ways of heat source other than solar, which is not applicable in the present study.

$$m_{water} = \frac{m_i(M_i - M_f)}{(100 - M_f)} \tag{11}$$

$$Q = m_{water}\, h_{fg} \tag{12}$$

$$\eta_{system} = \frac{m_{water}\, h_{fg}}{I_T A_c + E} \tag{13}$$

In recent times, artificial neural network (ANN) has evolved as useful computational software for modeling drying processes. Solar drying of various products involves various dependent variables such as radiation, temperature, humidity, etc. Researchers worldwide use the ANN tool for testing and validation of the drying performance of solar dryers. The ANN-based models can predict the heat transfer coefficient [17], moisture ratio, moisture content, or drying rate depending on the requirements and available parameters [18]. Compared to other theoretical and practical modeling methodologies, ANNs may have advantages in simulating these devices, including high accuracy, generalization ability, and quick data insights [19]. Despite the basic assumptions in ANN-based modeling, using ANNs reduces solving complex mathematical models. In addition, fewer experiments are necessary to determine the input/output linkages compared to experimental investigations. Consequently, time and money could be saved by system modeling using ANN. ANN processes the dataset fed into the system mathematically in the form of nodes/neurons. The model consists of input layers as the variables affecting the model, and the output layer is based on the output desired for the prediction. The researcher decides on the hidden layer of the model per the problem's intricacies. Training, validation, and testing are three stages of using ANN models. Training and validation stages involve both the input as well as target data. However, the testing is performed only with input data to see the model's suitability.

The dryer's performance largely depends on the final moisture content of the dried product. It is helpful for researchers to develop a model to predict final moisture through neural network simulation. Bala *et al.* predicted the performance of the solar tunnel dryer using a multilayered neural network technique [20]. The model was trained using a backpropagation algorithm utilizing data on the solar drying of jackfruit bulbs and leather.Similarly, the present study is designed for the wood biofuels. One hidden layer was selected in the model under Levenberg-Marquardt for training the mean square error regression in MATLAB2017b software. The Levenberg-Marquardt algorithm, which is created especially to minimize the sum of square error, is useful in similar predictions. As a first-choice supervised learning approach, the trainlm is frequently the quickest propagation algorithm in the toolbox, albeit it does use more memory than other algorithms [21]. It is applied in the current analysis. The model was trained with random data set from the experiments with 10,000 iterations with tan-sigmoid activation function for hidden neurons and purelin for linear output neurons. The test, train, and validation curves are presented in the results section. After several hits and trial runs the best performance curve was plotted. The dryer's performance largely depends on the final moisture content of the dried product. It is helpful for researchers to develop a model to predict final moisture through neural network simulation. Bala et al. predicted the performance of the solar tunnel dryer using a multilayered neural network technique [20]. The model was trained using a backpropagation algorithm utilizing data on the solar drying of jackfruit bulbs and leather. Similarly, the present study is designed for wood biofuels. Figure 2. depicting the ANN model developed for prediction of the final moisture content based on the experimental data collected

during the experiments mentioned in Table 2. The five input variables affecting the process were selected as solar radiation, inlet and outlet temperature, and relative humidity. One hidden layer was selected in the model under Levenberg-Marquardt for training the mean square error regression in MATLAB2017b software. The Levenberg-Marquardt algorithm, which is created especially to minimize the sum of square error, is useful in similar predictions. As a first-choice supervised learning approach, the trainlm is frequently the quickest propagation algorithm in the toolbox, albeit it does use more memory than other algorithms [21]. It is applied in the current analysis. The model was trained with random data set from the experiments with 10,000 iterations with tan-sigmoid activation function for hidden neurons and purelin for linear output neurons. The test, train, and validation curves are presented in the results section. After several hits and trial runs the best performance curve was plotted.

Table 2. Experimental parameter and their range considered for designing the ANN model.

Parameters	Range	Units
Solar Radiation	100-1100	W/m^2
Inlet Temperature	18-32	°C
Outlet Temperature	20-60	°C
Initial Moisture content (wet basis)	32-36	%
Final moisture content (wet basis)	16-28	%
Relative Humidity	25-75	%

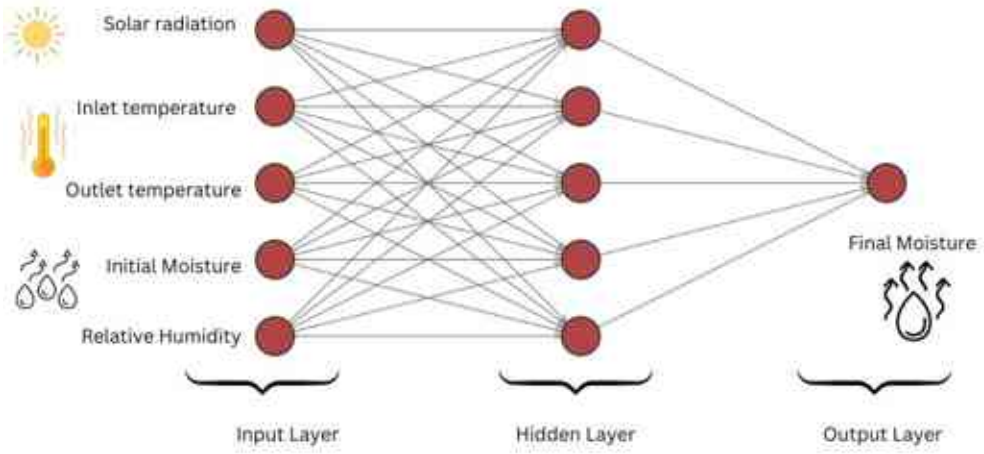

Figure 2. Pictorial depiction of the ANN model developed.

2.3.Methodology for Hybrid Solar Dryer

The cabinet dryer developed for this study is made up of wooden blocks as walls of the dryer. Figure 3. comprises the schematic illustration, where the working mechanism and the real-time pictorial view of the dryer are shown. It consists of three prime chambers, namely, the collector chamber for trapping hot air and its transmission with the help of an exhaust chimney fan. The

drying chamber (Length x Breadth x Height) is (80 x 50 x 45) cm in size and has three layers of trays consisting of one kilogram of the samples of woodchips, sawdust, and pellets each. Similarly, the bottom chamber below the drying chamber is for hybrid support of thermal energy coming out of the phase transition of PCM, i.e., Coconut oil. The volume of the drying chamber and the PCM material chamber is 180 liters. The airflow for drying occurs through six holes at the collector inlet of 2 cm diameter and three outlet holes in the drying/PCM chamber with a six cm diameter each. A power supply chimney fan circulated the hot air for consistent drying with an airflow of 2 m/s regulated using an anemometer.

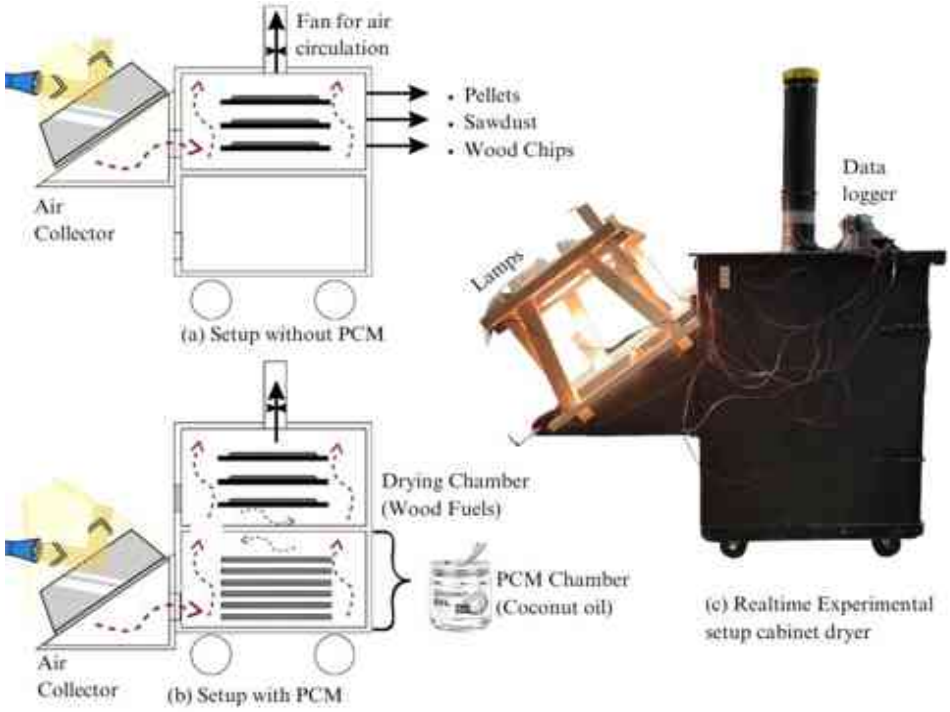

Figure 3. Schematic description of the (a) dryer without PCM chamber, (b) dryer with PCM chamber, and (c) real-time cabinet dryer pictorial view.

The collector was placed for the inlet airflow at the top for the "without PCM" scenario, as shown in Figure 3 (a), and at the bottom chamber only during the "with PCM" scenario of experiments, as shown in Figure 3 (b).

For two prime scientific reasons, it was decided to perform the trials with an artificial solar source (i.e., halogen lights) rather than outdoor environmental conditions. Foremost, because of alterations in weather and cloud cover, radiation levels during studies with the sun might fluctuate significantly during the day. The solar dryer's energy and exergy efficiency may fluctuate due to this unpredictability, making it challenging to gauge and contrast performance under various circumstances precisely. It is feasible to create an artificial sun that emits rays in a predictable and regulated manner, making it possible to evaluate energy and energy efficiency with greater accuracy and dependability. Secondly, a potential method for improving solar dryers' efficiency is using phase change material (PCM) for continuous drying. However, because of the variations in radiation levels, it might be challenging to assess PCM's efficacy in the normal sun. It is feasible to examine the performance of the solar dryer with and without PCM under constant and regulated settings by employing an artificial sun, giving a more precise evaluation of its efficacy.

In order to generate constant radiation for the air collector, four halogen reflector lamps of 500 Watts capacity were placed above the collectors with the help of wooden frames. Last but not least, using a halogen lamp offers a more regulated and reproducible experimental setting, enabling more precise and trustworthy evaluations of the effectiveness of the solar dryer. This can enhance the study's scientific rigor and boost trust in the findings.

In order to better understand how PCM might be applied to solar thermal devices such as solar heating systems, dryers, greenhouses, etc., many empirical forms of research have been performed. Research shows that the performance of all applications, in most cases, improves using PCMs. A technology that has greatly benefited from this is the combined PV-Thermal systems (PVT), with some sources reporting an impressive increase in the overall efficiency of over 40% [22]. For temperatures above 20°C, coconut oil PCM, coconut oil nano-PCM, and coconut oil nano-PCM embodied in metal capsules can be utilized as temperature regulators. While the latent heat discharging process occurs at a relatively low temperature of (16–18°C), the latent heat charging process occurs between 20–25°C. Therefore, it should be possible to extract this latent heat during the night hours of drying to supply continuous heat to the dryer. Coconut oil is non-corrosive to metal containers, has a comfortable melting point, a high latent heat capacity, and has little to no supercooling during the phase change process. One of the many instruments used by researchers to verify various kinds of organic and non-organic phase change materials is differential scanning calorimetry (DSC). Data on the melting temperature, freezing temperature, latent heat, and specific heat capacity are typically collected using DSC measurements. These parameters are vital in understanding the performance of the PCM as a TES media [23]. Safira *et al.* [24] investigated the thermal properties of coconut oil based on DSC studies for building energy storage applications. The experiments involved examining the addition of graphene that affected the thermal storage properties of the samples. Figure 4 is a modified schematic of the experimental results of this study depicting the two crucial phases of the solidification and melting of the coconut oil. The area under the curve can be used to calculate the latent heat of melting or solidification based on the endothermic or exothermic reactions. Though coconut oil as PCM is cheap and readily available, its performance as a thermally efficient PCM is not yet explored extensively. The energy assessment of the dryer "with" and "without" will reveal the utility of coconut oil as a potential PCM for the solar drying of wood fuels. Some of the critical characteristics and thermal properties of coconut oil are mentioned in Table 3.

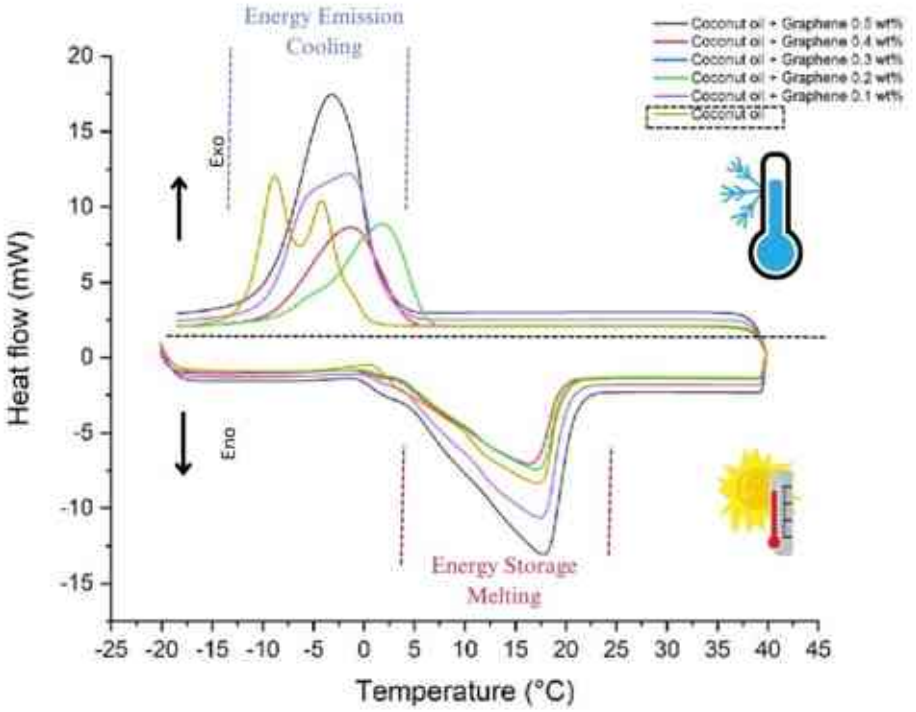

Figure 4. DSC curves of coconut oil during the phase change transformation (Recreated from source: [24]*).*

Table 3. Thermal properties of coconut oil used in the investigation [25] [26] [27].

Thermal Properties	Coconut Oil	Air
Density (Kgm^{-3})	916	1.137
Melting Point (°C)	22-26	-
Heat of Fusion ($kJkg^{-1}$)	103.25	-
Thermal conductivity ($Wm^{-1}K^{-1}$)	0.161	0.0024
Specific heat ($kJ\ kg^{-1}\ K^{-1}$)	0.62+0.1006 T	-
Viscosity (cSt)	20	-
Moisture content ($mgkg^{-1}$)	1	

In this section, investigations on the thermal efficiency and exergy of wood fuel drying systems using phase change material are discussed. Specifically, woodchips, pellets, and sawdust are used as our sample wood fuels and compared their drying performance using the proposed hybrid solar dryer with the performance of an open-sun drying system. Historically, waste streams from timber and other industries have formed the backbone of processed wood fuels. However, in recent years, the production of wood chips, pellets, and sawdust fuel for blending with coal have entirely relied on fast-growing tree crops [28]. Considering the high demand [29], it is inevitable to maintain the moisture content of these wood fuels [30]. The goal was to propose an economically viable and environmentally sustainable drying solution for industrial applications. During charging and discharging cycles, phase-change materials like coconut oil can store and release thermal energy [25]. The PCM is heated throughout the charging cycle, changing from a solid to a liquid phase and absorbing heat in the process. This cycle is influenced by temperature since hotter temperatures enable quicker and more effective charging. When the liquid oil cools down

throughout the discharging cycle, it solidifies, releases the heat trapped inside, and becomes usable. Temperature also influences this cycle since slower and less effective heat release occurs at lower temperatures. A heat storage medium, such as a micro [31] or macro [32] encapsulate that can absorb and transfer the released heat to a desired location or process must be placed optimally to extract latent heat from the PCM. The heat that has been stored can be used in this way. The proposed hybrid solar dryer consisted of a drying chamber with three layers of one-kilogram samples of each wood fuel product and an additional bottom chamber with eight layers of PCM trays. A data logger with K-type thermocouples recorded the temperature data throughout the experiment. The current study focused on improving energy efficiency and evaluated the economic and environmental performance of the proposed drying system.. Furthermore, to evaluate the environmental impact of the proposed system, the reduction in carbon footprint was measured and compared to the open-sun drying system, as shown in Figure 5. The three kinds of wood fuels were acquired from a local supplier in Miskolc, Hungary. The sample fuels were kept for 24 hours with sprinkled water to observe the moisture.

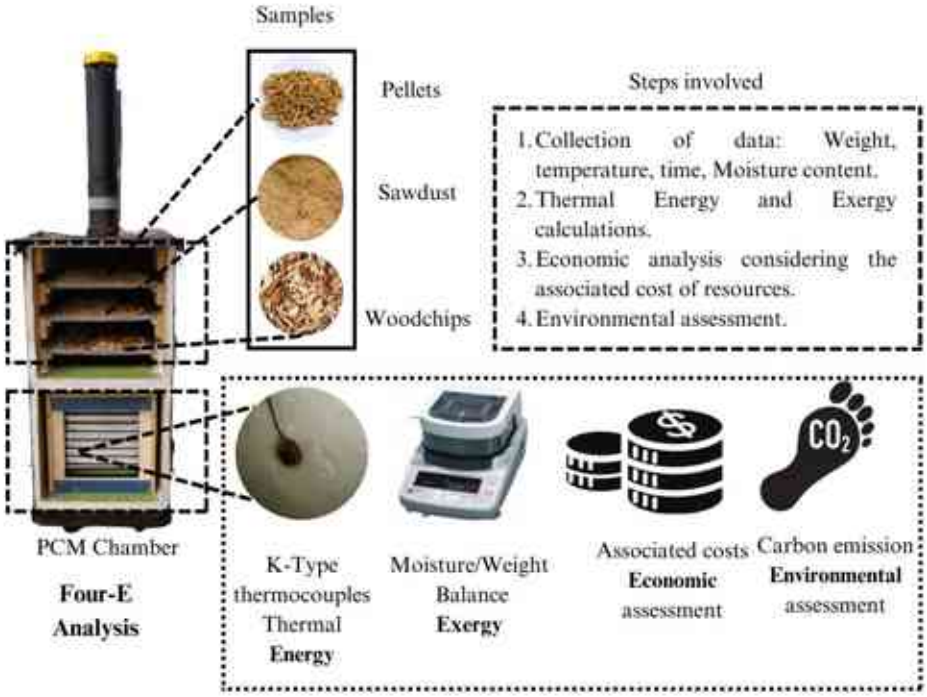

Figure 5. The four-E (Energy, Exergy, Economic and Environmental assessment methodology adopted for the present study.

The moisture content was measured on the moisture balance machine (readability of 0.001 grams). The initial moisture content was measured as 45%, 37%, and 39% for wood chips, pellets, and sawdust samples, respectively, on a wet basis. Four (DELL082) Halogen reflectors of 500 Watts were used as the radiation sources. Xenon lights could also be used for such experiments but were not used due to unavailability in the local market. The pyranometer (SOLART-SYS) was used for irradiance measurement, and the instrument had a sensitivity of ±0.1 mV/Wm2. After measuring the moisture, air velocity, and irradiance, the three samples were measured for one-kilogram samples on a weighing machine (sensitivity ±0.1 grams). These samples were then placed, and the drying of the samples was observed for a duration of 22 hours. This period was selected because, after 20 hours, the system's temperature returned to normal since the lamps got switched off. The

four-E analysis is performed from these observations to understand the feasibility of solar drying of wood fuels.

For optimal effectiveness, it is crucial to comprehend solar dryers' thermal energy and exergy efficiency. The quantity of energy used efficiently to dry the product in a solar dryer is determined by thermal energy efficiency. One can assess the effectiveness of the solar dryer in converting solar energy into usable heat energy for drying by knowing the thermal energy performance. These experiments can assist in improving the solar dryer's construction to increase utility and decrease energy losses for drying wood biofuels.

On the other hand, exergy efficiency describes the solar dryer's energy caliber. Exergy determines the most useful work that can be done with the energy by accounting for the irreversibility in the system, such as heat losses from convection and radiation [33]. In previous investigations, authors performed experiments for the wood biofuels in open weather conditions for open sun drying [34], box-type natural convection drying [35], and forced convection drying in cabinet dryers with open sun and varying radiation conditions [36]. Understanding exergy performance allows one to assess the caliber of the energy consumed and locate opportunities for exergy loss reduction, both of which contribute to the system's total effectiveness. Simultaneously, conducting an economic analysis of solar drying of wood fuels can offer essential insights into the production and dissemination of wood biofuels and assist in developing more efficient and sustainable techniques for their production.

3. RESULTS AND DISCUSSION

3.1. Results of experimental investigations- Open and Box-type dryer

During experiments, various shapes and sizes of the wood chips of grade EN14961 were used in the laboratory. EN14961 is the European grade of solid biomass fuel utilized for various industrial as well as Non-industrial applications. The moisture content measurement was done using a lab-scale moisture measuring instrument. These woodchips are readily available around the forest regions of Miskolc city. The woodchips were pre-soaked for 24 Hrs before sun-drying the chips in a box-type dryer developed at the laboratory.

To understand the wood chips' drying nature, different sizes of the wood chips were kept under observation. The experiments were conducted in November, 2021, when the ambient temperature at the city of Miskolc fluctuated between 10 °C to 25 °C. The observations were made only for 20 days when the sunshine was good with a clear sky and the 4 best days with high irradiation were considered. It was recorded that the maximum temperature reached during the tests was 35 °C at the outlet on Day 1. The temperature profiles reveal that the maximum temperature attained inside the dryer was in the afternoon from 12 PM to 2 PM. As shown in Figure 6 and Figure 7. The temperature drops fast as the sun gets down in the evening. Hourly change of solar radiation also affects the drying phenomenon.

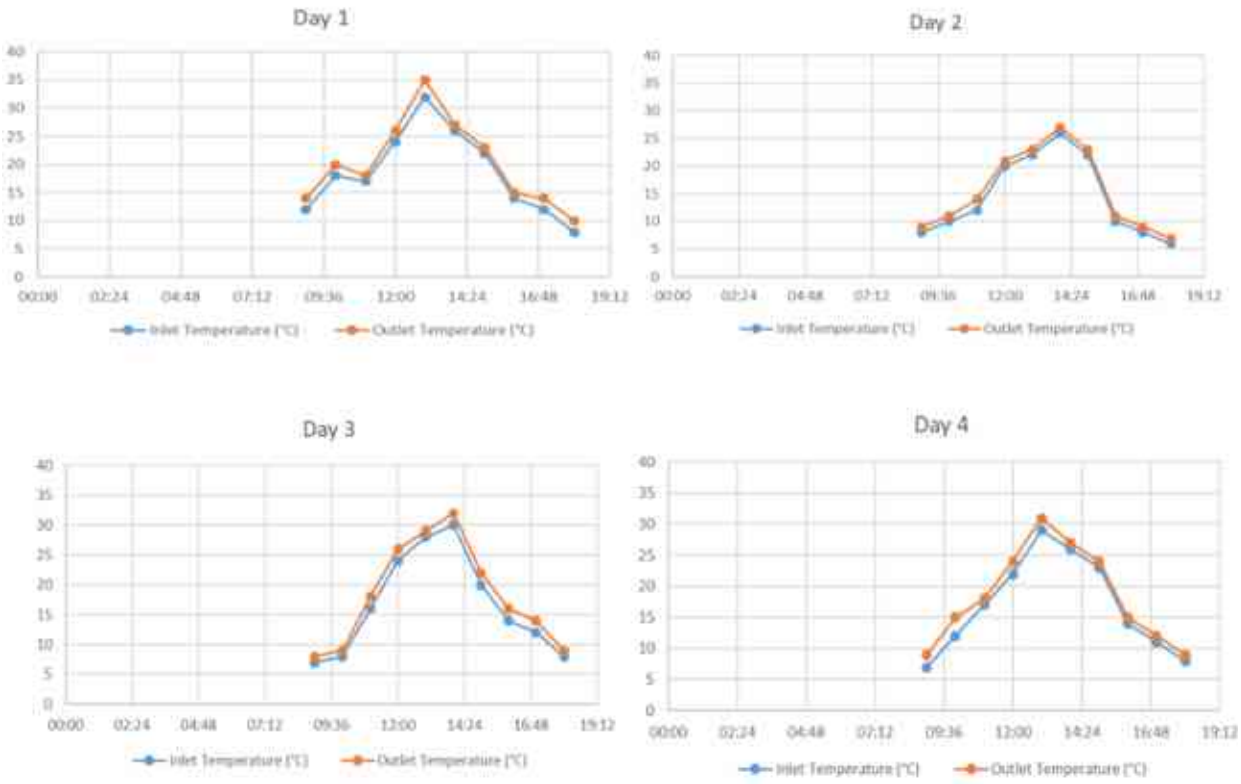

Figure 6. Temperature profiles of the inlet and outlet temperatures at the different days of the experiments.

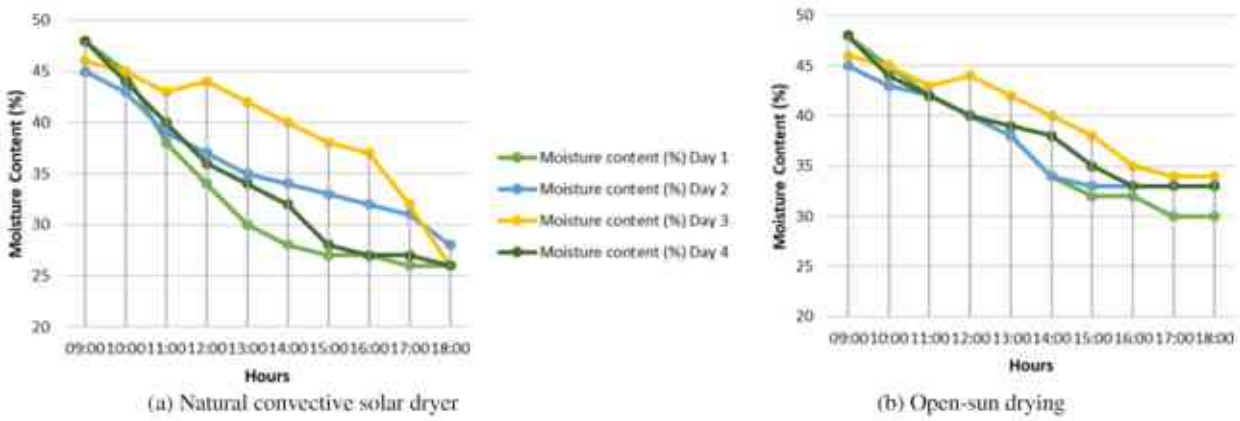

Figure 7. Moisture content graph of wood chips for (a) Natural covective solar dryer (b) Open sun drying.

3.2. Results of experimental investigations- Cabinet dryer

The experiments were performed at the University of Miskolc, Hungary, on twenty sunny days in October 2022 and the best irradiation days were considered as three days. The solar radiation measurements reflect the consistency of average radiation above 600 W/m2. However, sudden drops can be seen in the graph of Figure 8. The radiation values dropped suddenly because of the cloudiness or low sky-clarity index. Among the three-day experiments, the third day recorded the highest radiation value of 1100 W/m2. The consistency in good solar radiation helps in the rapid

rise of temperature inside the collector and drying chamber, leading to better drying rates for the solar dryer.

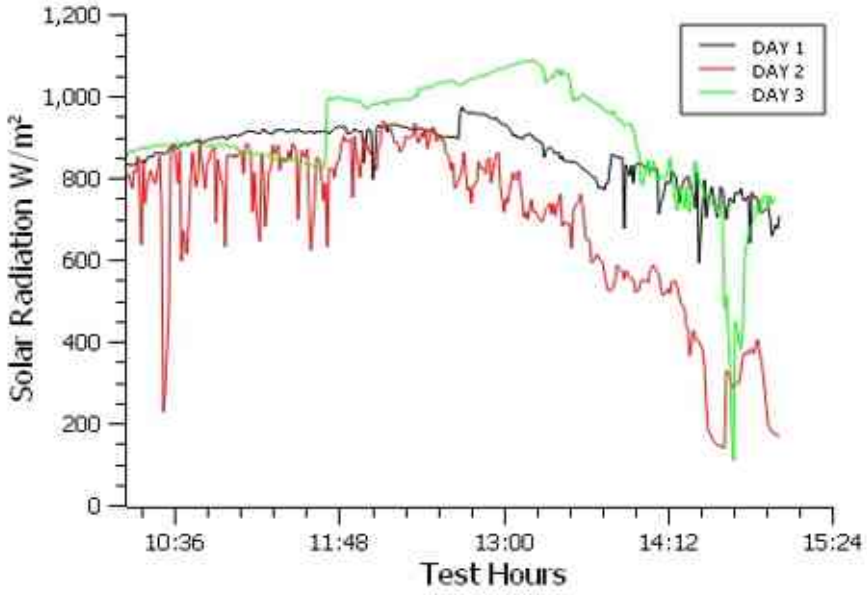

Figure 8. Solar radiation data collected for the three-day experimental setup.

Temperature rise is critical in the drying of agricultural products. The data logger and K-type thermocouple sensors were installed in the system at different locations. The collector's inlet and outlet temperature determine the air collector's efficiency. Considering no losses due to good insulation, the outlet temperature of the collector is the inlet of the drying chamber. In the three-day experiments, the maximum temperature achieved was 60°C at around 1100 W/m2. The complete temperature rise was observed between 12-2 P.M. During total experimental hours, the temperature gradient between the ambient and inside the chamber was around 10°C, which aided in the continuous drying of the wood products. There was little temperature difference between the top layer and bottom layer of the drying chamber. However, the RH value differed by 4-5 % occasionally. Figures 9, 10 and 11 represent the temperature profile of the system for the testing hours during Days 1,2 and 3, respectively.

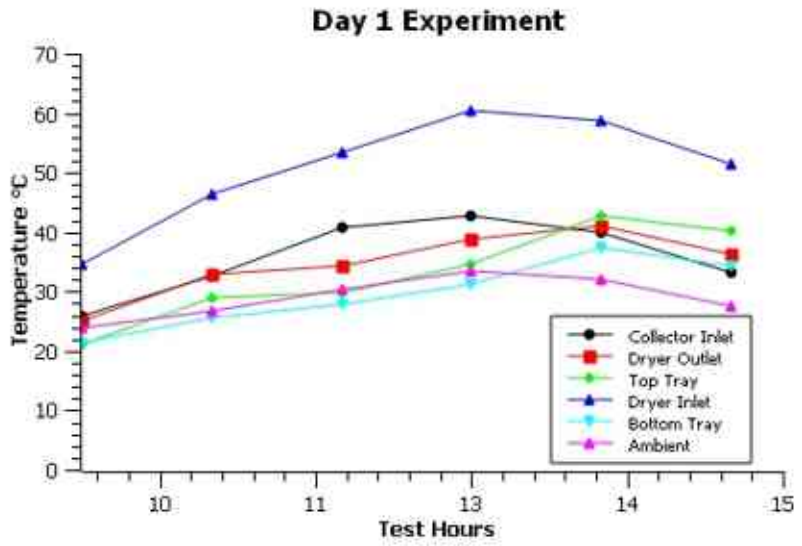

Figure 9. Temperature profiles for the first-day experimental setup of the dryer.

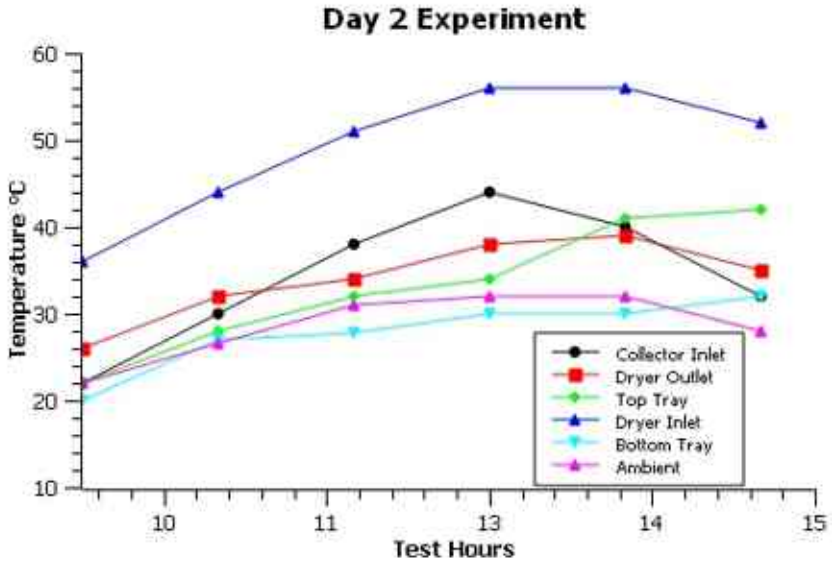

Figure 10. Temperature profiles for the second-day experimental setup of the dryer.

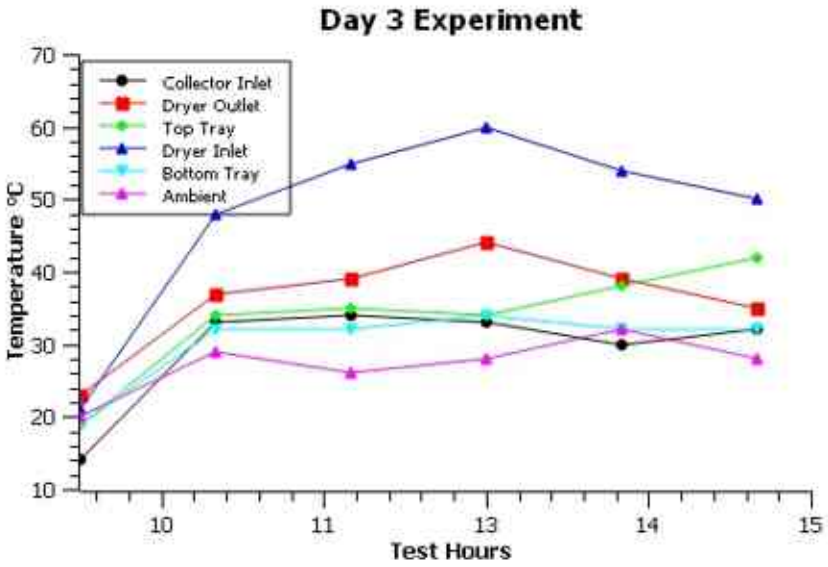

Figure 11. Temperature profiles for the third-day experimental setup of the dryer.

The instantaneous thermal efficiency of the air collector ranged 14.77% to 55%, as shown in Figure 12. The ambient temperature fluctuated between 18-32°C. The thermal efficiency dropped between 11 A.M. and 1 P.M. However, the efficiency constantly rose after that period. The possible reason could be temperature stability was achieved during this period. Figure 13. Depicts the variation of useful heat gains Qu of the solar collectors and the ratio of the change in temperature (ΔT) to solar radiation (°C m2/W) with the drying time of the experiment. The ratio of (ΔT) to solar radiation (°C m2/W) was used as a basis to compare the trend shown in 14. The hourly heat gain Qu range was recorded as (201.65 - 420.55) Watts. The total heat gain sum for Day1, 2 and 3 is 1495.57, 1663.62 and 2050.13 Watts, respectively.

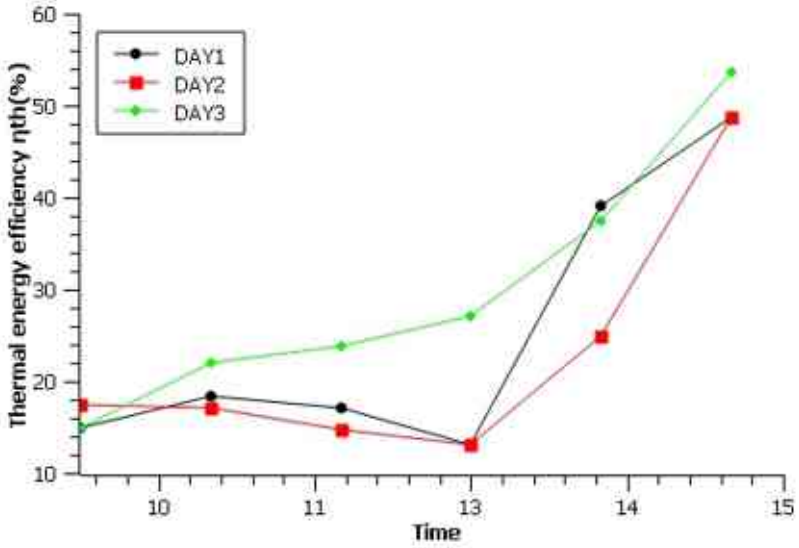

Figure 12. Thermal energy efficiency calculated on an hourly basis for the three-days.

The exergy gain and the exergy efficiency calculations are critical in understanding the thermal performance of the air collector. The performance of the drying chamber is directly proportional to the collector's performance. The energy utilized or the gain improved from morning to afternoon

hours is indicated in Figure 13. The value of exergy gains enhanced from 76.26 Watts to 408.57 Watts during the experiments in Figure 14. The exergy efficiency improved significantly from 4.8 % to 51.1 % from the first to the last hour, respectively. In addition, the Moisture ratio trends for the three wood fuels are plotted in Figure 15. The rapid loss of moisture content is evident in the wood pellets and sawdust samples. The high porosity level in these two fuel forms aids the fast internal migration of the surface water from the wood fuel. At the same time, the woodchip's surface water evaporation takes place slowly. Also, better exergy and long hours of continuous during can provide better results and insights on the drying behavior. The relative humidity (RH) measured for the samples during early hours was as high as 75%. However, the RH values kept fluctuating at the three levels of the tray primarily because of the different nature and drying rates of the three wood fuel samples.

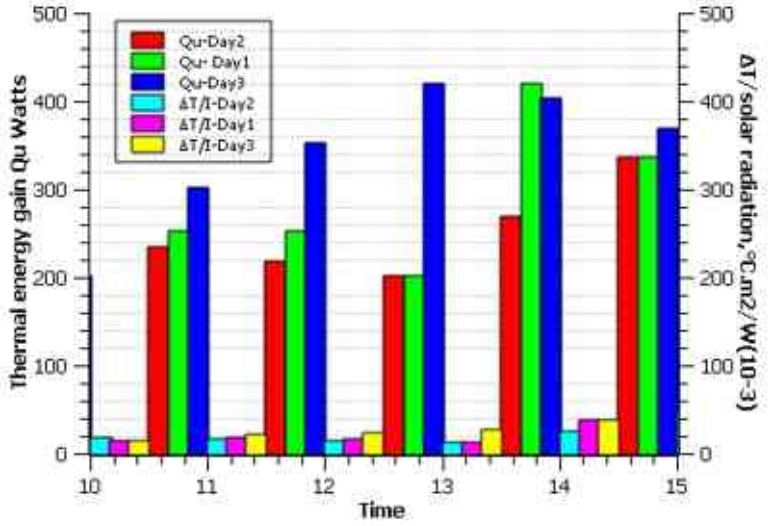

Figure 13. Thermal energy gain and the ΔT/solar radiation are calculated on an hourly basis.

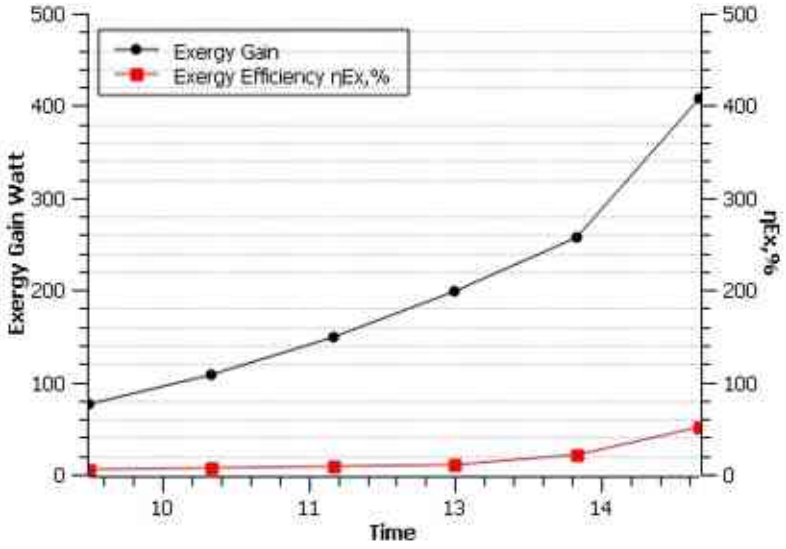

Figure 14. Exergy gain and Exergy efficiency are calculated on an hourly basis.

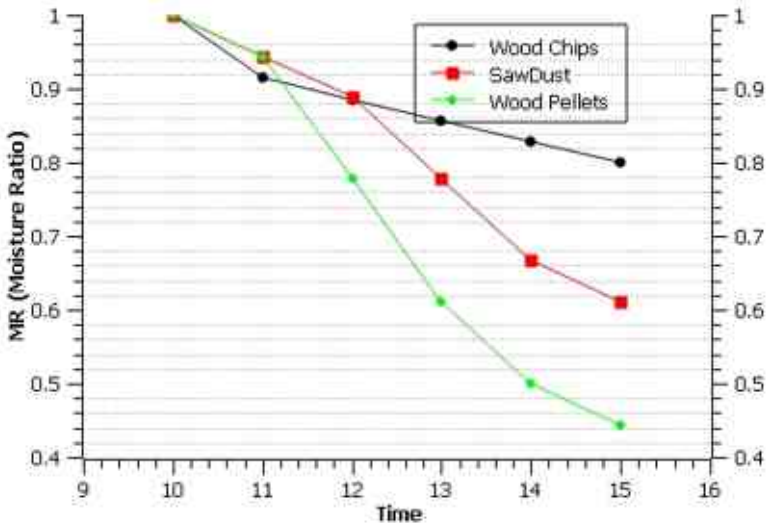

Figure 15. The moisture ratio was calculated for the wood chips, sawdust, and pellets.

The ANN model was employed in the NN-tool of MATLAB software to validate and predict final moisture content. The Coefficient of correlation (R) gives the goodness of the model. The training, validation, test, and overall values were found to be 1, 0.995, 0.970, and 0.990, reflecting the confirmation of the model shown in Figure 16. The predicted values were found to be coherent with the experimental dataset. The training was completed in 2nd iteration when the validation samples of mean square error reached the optimum value. The best validation performance was 2.4949 at epoch 993, where the epoch measures the number of times all training vectors are used once to update the weights.

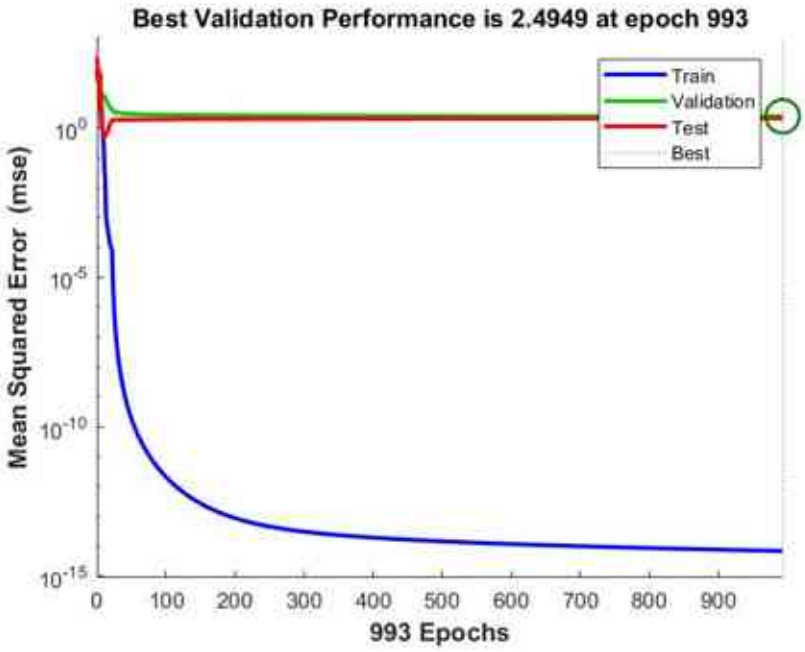

Figure 16. Root mean square error (MSE) plot for the ANN model.

In the above model, (ANN) is employed to forecast the performance of combined solar dryer. While ANN has previously been applied to predict drying performance in fruits, vegetables, and various agricultural/biomass products, its application to wood fuels is a novel contribution highlighted in this research. Notably, the model is highly adaptable, allowing for modifications in

input vectors, target vectors, and weights to fine-tune predictions for specific drying conditions, thus mirroring the presented model's versatility. An impressive achievement of this study is the development of an ANN model with a remarkably high R-squared (R2) value of 0.99, signifying its exceptional precision in predicting moisture content. Furthermore, this adaptable approach holds promise for predicting an array of other critical drying parameters, such as solar radiation, moisture ratio, and heat transfer coefficient, underscoring its potential for wide-ranging applications in the field.

3.3.Results of experimental investigations- Hybrid Dryer

The present work attempts to understand the role of constant radiation supply in the two scenarios (with and without PCM). The collector size had a limitation to fit four lamps on top of it. Hence, the maximum radiation achieved was 755 W/m^2 by placing it at a distance of 1.5 meters on top of the collector. The size of the collector and the radiation may vary for large-scale practical applications. In Hungary (city Miskolc), where the experiments are conducted, the value of the global radiation at midday throughout the winter half-year (from October to March) ranges between 250 and 600 W/m^2 . It is between 600 and 1000 W/m^2 from April to September, which is the summer season making the radiation value of 755 W/m^2 nearly realistic with a fixed mass flow rate of 0.016 kg/s for both scenarios, i.e., (with and without PCM).

The radiation of 755 W/m^2 was maintained during the experimental hours (charging period) between 10 A.M. to 1 A.M. of the post-day. After 15 hours, the lamps were switched off to observe the dryer's behavior during the PCM's discharging period. During experiments, the temperatures were measured constantly through the data logger and temperature sensors. The hourly temperature distribution of the dryer is plotted against time and radiation in Figure 17 (a) without PCM and Figure 17. (b) with PCM. The radiation curve, which drops suddenly at 1400 hrs., is due to the switching off the halogen lamps. For both conditions, the highest collector outlet temperature achieved was around 70°C and drops to 18°C in just three hours from (15:30 hrs to 18:30 hrs) at the outlet of the collector box. The ambient temperature remains constant at about 18°C for both (with and without) scenarios. For the without PCM experiments, the temperature profile of all sensors slump rapidly to lower temperatures as observed in Figure 17 (a) and 17(b).

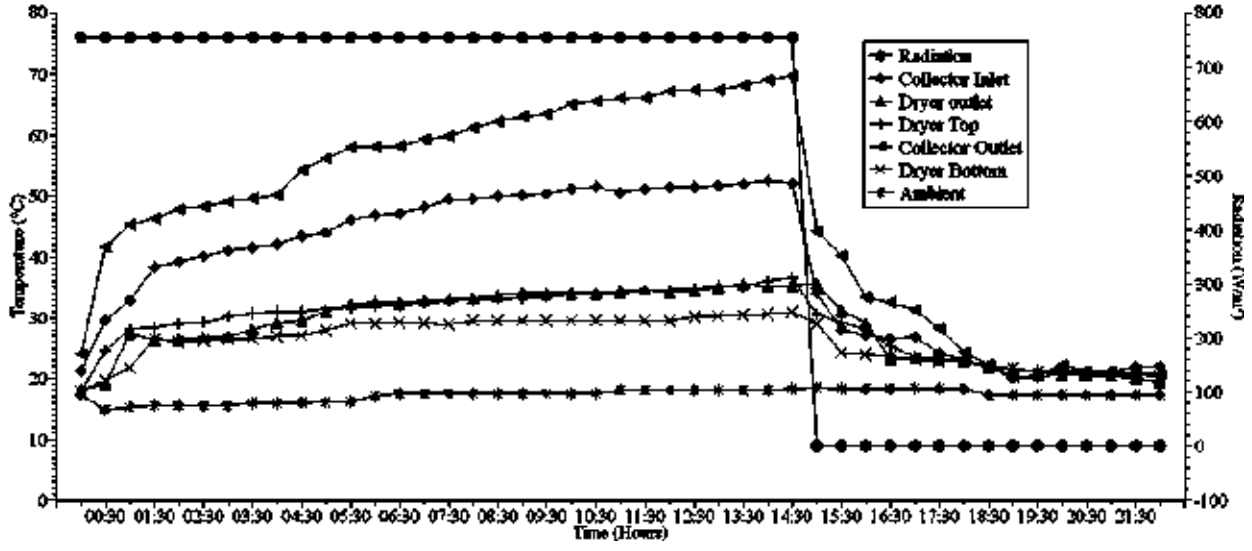

Figure 17 (a). Temperature and radiation profiles during experiments without PCM.

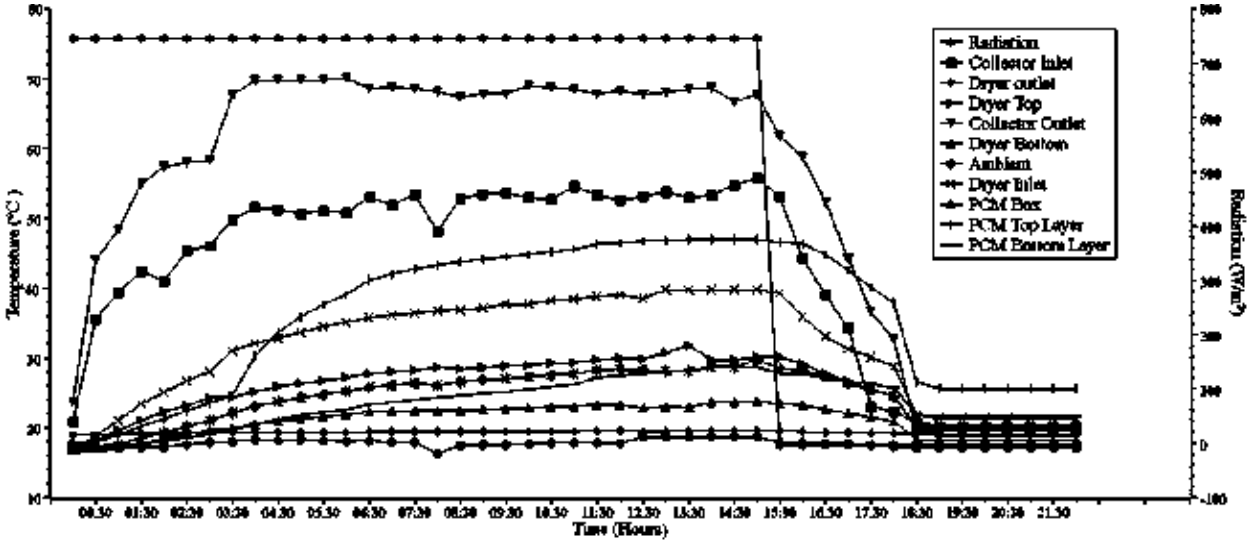

Figure 17 (b). Temperature and radiation profiles during experiments with PCM.

On the contrary, in the PCM condition, as the coconut oil solidifies and releases the stored energy, the slump in trend is not observed, and the various parts of the dryer retain some heat. The collector outlet temperature gradually lowers from 15:30 hrs to 18:30 hrs (from 70°C to 25°C). The temperature was deprived gradually and reached below 30°C after 3 hrs of switching off condition compared to without PCM condition where it goes down 30°C just after one hour. After the first three hours, the dryer outlet, i.e., near the chimney, was maintained at above 40°C (without PCM) while it was above 50°C until switching off condition. In similar research on the solar drying of wood, Tagne and Azese developed a dryer with thermal energy storage at two locations in France. The maximum air temperature achieved was 78°C. Another solar greenhouse dryer developed by Alberto et al. for drying woodchips attained a maximum temperature of 59.9°C with a temperature gradient of ambient and inside as 25.2°C. Also, with a black pebble bed as thermal energy storage for drying timber, the maximum temperature achieved was 61.7 °C [11]. This observation reflects the performance of coconut oil as a notable potential heat storage material. However, it's also crucial to calculate the energy and exergy performance of the dryer during the experiments, which are discussed in further sections.

When evaluating the efficacy and cost-effectiveness of the system, it is crucial to consider the energy gain and energy efficiency of a solar drier. The solar dryer is more desirable for drying applications due to higher energy gain or efficiency, resulting in faster drying rates, more drying, lower energy usage, and smaller system sizes. The thermal performance of the dryer was evaluated with and without PCM conditions, as shown in Figure(s) 18 (a) and 18 (b). It observed that the useful heat gain was prolonged with some amount of heat (300 Watts) until 18:00 hours as the temperature gradient was maintained. During the PCM discharging (solidification), the PCM retains some amount of heat (300 Watts) for 3-4 hours, and then as the temperature gradient nullifies, the efficiency slumps down.

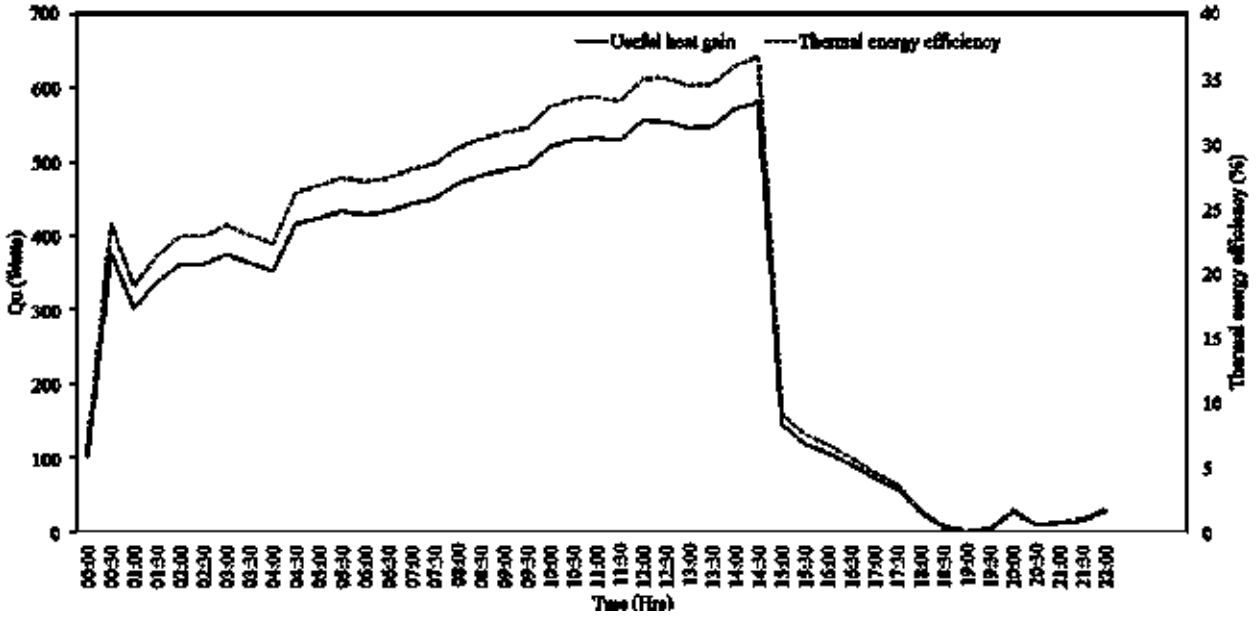

Figure 18(a). Useful heat gain and thermal energy efficiency against time (without PCM).

For the without PCM condition, the sudden surge can be observed in Figure. 18 (a) with a heat gain of up to 600 Watts and maximum efficiency of 37%. During the PCM Figure. 18 (b) experiments, the heat gain remains steady and below 600 Watts, and efficiency remains between 30 and 35%. However, the efficiency steadily drops to below 10% only after 3-4 hours after the radiation is turned off completely. The energy efficiency during the four hours of heat retention in the case of PCM, the efficiency increases by 63.64%. In general, studies [11] and [36] suggest that the energy efficiency of solar wood dryers is in the range of 30 to 40%, thereby validating the utility of coconut oil and hybridization of the dryer.

Figure 18(b). Useful heat gain and thermal energy efficiency against time with PCM.

Exergy analysis is frequently used to pinpoint inefficient and energy-wasting areas in a system and to improve its setup and operation for optimum energy effectiveness. Exergy values in a

system may fluctuate due to several variables, including temperature, pressure, flow rate, component effectiveness, and irreversibility. Optimizing the functionality and effectiveness of energy exchange systems requires a thorough understanding of these variations and their underlying causes. Figure 19 (a) reflects that during the experiments without PCM, with highest exergy efficiency between 14.4-14.5% and drops down to below 30% during off radiation hours.

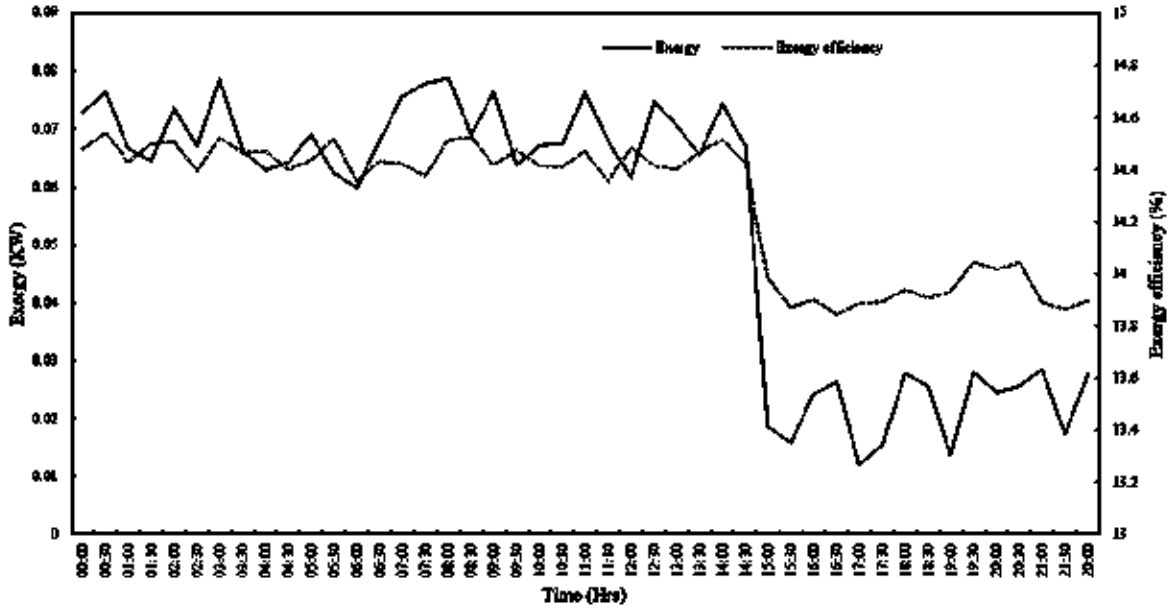

19(a). Exergy gain and exergy efficiency against time without PCM.

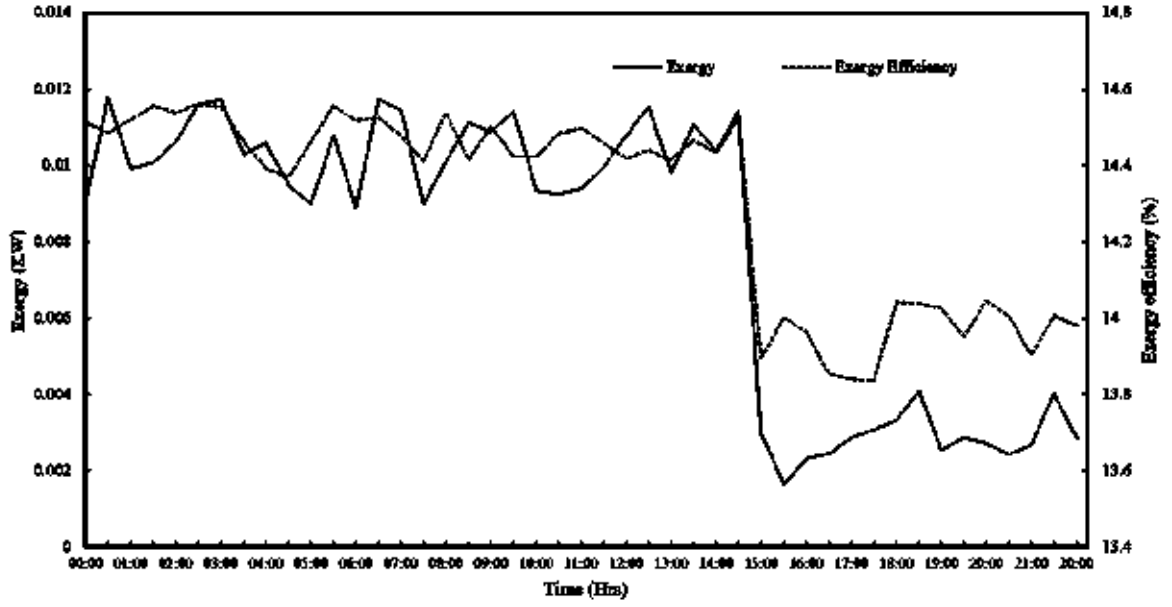

Figure 19(b). Exergy gain and exergy efficiency against time with PCM.

Conversely, for the with PCM experiments, the exergy efficiency fluctuated between 14.1 14.6% during the charging period of PCM and slumped to 13 13.9% during the discharge period of PCM. The exergy was much higher, with PCM conditions reaching 0.012 kW. The fluctuations observed in Figure. 19 (b) could be due to pressure variation between the PCM storage chamber

at the bottom and the drying chamber of the samples. In the large-scaleindustrial drying of wood chips, the drum drying system (DDS) (conventional dryer) with capacity ranging between 10 and 180 t/h (wet product). With the temperature rising to 260°C, the energy and exergy efficiencies were calculated as 34.07% and 4.39%, respectively [112]. However, limited research covered the exergy aspect while designing/developing solar-based drying systems specifically for wood fuels. It is important to note that the drying material's thermal and chemical properties influence a solar drying system's exergy efficiency. The exergy efficiency of drying might vary depending on the material's composition, moisture level, and specific heat capacity.

The conclusions of the economic study were informative. The considered solar dryer with a ten-year lifetime and a 12% interest rate has a CRF of 0.172. This indicates that the capital investment's equivalent yearly cost is 17.2% of the initial investment. Researchers may compare the cost of the solar dryer to other drying techniques by using this CRF value to determine the yearly cost of the solar dryer, which includes both capital and operational expenditures. For the entire experimental setup, our initial capital expense was 279 EUR (Euros). As a result, it was determined that the fixed annual cost (FAC) of the solar dryer is EUR 49.38, reflecting the equal yearly cost of the capital investment over the dryer's anticipated lifespan, considering both capital and operational expenses. Further, the sinking fund factor (SFF) calculates how much money must be placed away a year, assuming a particular rate of interest, in order to amass a specific amount of money over a specific amount of time. Based on this, the ASV was found to be 3.18 and the AMC to be 7.42. Metallic macro-encapsulates with organic paraffin wax (PCM) can also be used as short-term energy storage inducing thermal lag in solar drying systems. Research shows that the double-pass air solar heater system is economically feasible for solar drying operations. This system's associated ASV (annual salvage value) and AMC (Annual maintenance operational cost) were found to be 3.13 and 7.31, respectively. The payback period for this dryer setup is calculated as approximately five years. The payback period depends on the interest rates and associated costs and savings. Literature suggests that this period could be as low as six-nine [113] months to as high as 4.69 years, per recent review recommendations . Also, the capital cost of solar dryers mayvary from 100 to 2000 US dollars, with a lifespan of 10-25 years [89]. A compilation of the calculated economic parameters is shown in Table 4.

Table 4. Calculated values of economic parameters (EUR)

Parameters	CRF	IC	SV	FAC	SFF	ASV	AMC	AC
Values	0.177	279	55.8	49.38	0.057	3.18	7.422	53.62

Considering the radiation value of 755 W/m2 and the working hours as 10 hours for those without PCM case and 15 hours for those with the PCM case, the average thermal efficiency is considered as 30%, and the number of working days is 150 days. The energy payback time (EBPT) calculated without the PCM condition is 4.03, whereas with PCM is 3.08. Research shows that energy payback could be critical in finding the best suitable hybridization of solar dryers. For instance, Saini et al. [115] evaluated a greenhouse solar dryer under forced mode integrated with four different types of photovoltaic (PV) technologies. The EBPT ranged from (0.39-1.13), and the lowest EBPT combination was proposed as the best feasible model. The low EBPT value of with PCM scenario in our study thus justifies the utility of PCMs for efficient drying conditions

of wood fuels. The CO_2 emissions per year, considering a lifetime of 5 years, is calculated as 64.09 kg per year. Similarly, with PV hybrid models, CO_2 emission (in kg) was found to be in the range of (40.96-141.73) kg [115]. The specific energy consumption was calculated considering the wet basis average final moisture content of 15% to average initial moisture content of 45%. The SEC is estimated as 5.22 kWh/kg, which, in the case of the v-groove double pass solar dryer, was calculated as 3.096 kWh/kg. Considering the average exergetic efficiency of 50 %, the sustainability index was found to be 2, which in the case of wind-generated eco-thermal hybrid dryers was (1.28-2.5). The improvement potential (IP) shows the amount of a system's energy losses. The potential for improvement for various solar dryers varied from 0.047 to 0.094 kW [116]. The lack of productivity (LOP) was 6.85 and the IP as 0.058 kW, which falls under recommended range.

3.4. Results of trendline assessment of solar potential in Hungary and its neighbour countries

There are certain parameters which affect the solar PV potential analysis of any country or region. Among the several factors the solar irradiance, temperature profiles, weather conditions play a significant role [37]. Understanding the regional potential of PV-based energy generation geographical maps and thermal profiling could be an important tool in making accurate predictions for the region's energy capability [38]. Site-specific irradiance forecast supported with temperature profiling helps in understanding the forecast for PV regional potential. The sum of the energy falling on a surface on earth for a given time period is called Irradiation. The power or instantaneous energy rate received by a surface area on earth is known as Irradiance and is generally calculated on an hourly basis. The irradiance is correlated with cloud cover predictions. Thus, correct analysis of irradiance can be considered in compliance with the sky cover [39]. To understand the irradiance distribution of the visegrad countries, the PV-GIS interactive tool was used to observe the distribution in four countries [40]. The capital cities, namely Warsaw, Bratislava, Prague and Budapest, were considered irradiance in the respective countries. The Figure 20. gives a brief estimation of horizontal and direct irradiance values in the four countries over the period of 2005-2016. The Monthly solar radiation data analysis reveals that the irradiance of Warsaw, Bratislava, and Prague lies below the range of 200 kwh/m^2 even during the peak value months. On the contrary, for Budapest, Hungary, it could be observed that during the peak irradiance months, the values cross the range of 200 kwh/m^2 .The evident higher values reveals higher solar potential of the Hungarian region.

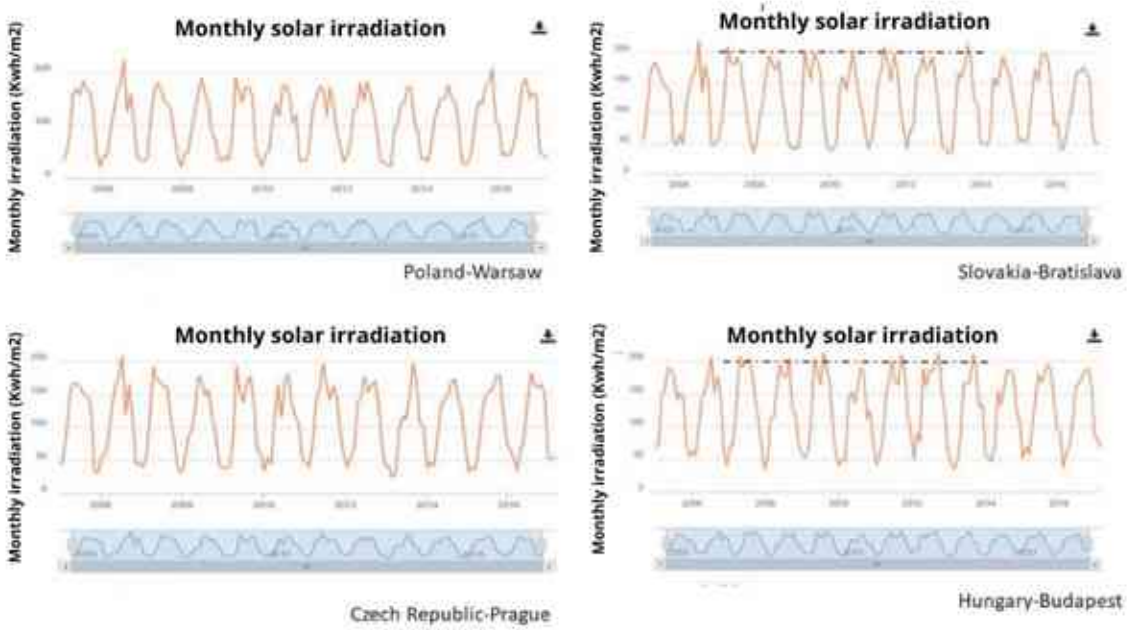

Figure 20. Solar Irradiation trendline of monthly values in capital cities of visegrad countries (2005-2016) [40]

Along with Irradiation data performance of grid, connected PV systems also play an important role in analyzing solar potential. European commission PV-GIS tool gives a monthly energy output for a fixed angle PV system. Figure 21. gives an estimate of energy output throughout the year in kWh. We analyzed the capital cities of the four nations on their respective capital cities. It can be seen that Bratislava (Slovakia) and Budapest (Hungary) gives an output of more than 125 kWh during the peak summer. Whereas for Warsaw (Poland) and Prague (Czech Republic) somehow managed to reach the output of 125kWh during summer. The analysis is based on database of PVGIS-SARAH with slope angle of 35 Degrees. Figure 22. shows solar park presence in various regions of Hungary based on power capacity. In that picture is also highlighted area with higher potential and with lesser solar parks

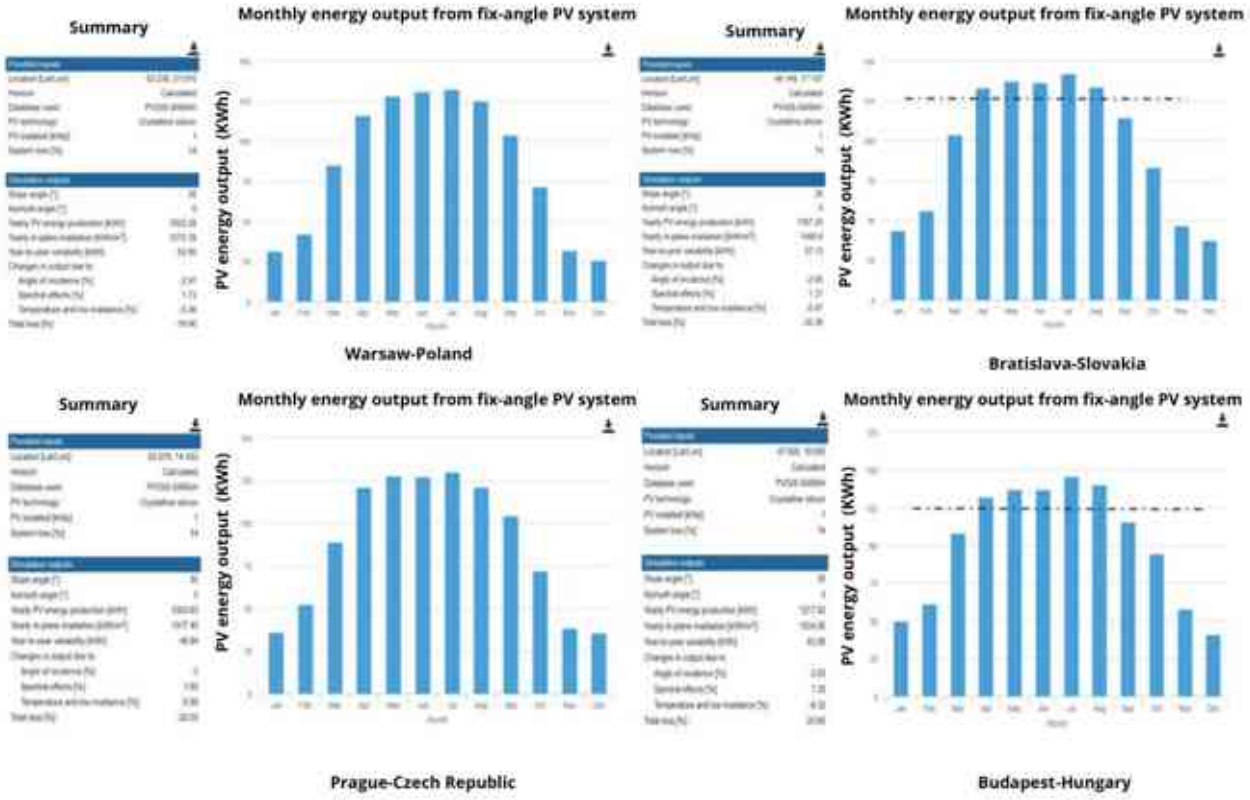

Figure 21. Performance of Grid-connected PV with energy output from fixed angle PV system in the capital cities of Visegrad Countries [based on the European Commission PV GIS analysis tool updated in 2019] [40]

Figure 22. Solar park presence in various regions of Hungary based on power capacity.

4. CONCLUSION

Energy and exergy efficiencies of the drying system are crucial, yet only a few studies on wood fuels considered calculating them. A few works with their distinct hybrid configuration and outcomes are presented in Table 5. Wood fuels as raw materials usually contain around 60% of wet basis (wb) moisture, and ideally, good quality fuels should be in the range of (5-15)% of moisture content (wb). Alberto *et al*. [41] studied solar greenhouse drying with samples of (Pinus pinaster) 2.68 cm half-length having an average initial moisture content of 50% kept in two piles. Solar greenhouse dryers were found to be more effective than open-air drying when drying was accomplished quickly and thoroughly by balancing the moisture content of the wood chips with the moving air. This implies that within the first 24 to 48 hours of drying, the moisture should be reduced to levels that are close to 30%. The present study results reveal that for around 22 hrs of consistent drying time, a significant drop of 34%, 29%, and 31% moisture content (wet-basis) was observed for woodchips, pellets, and sawdust, respectively. To achieve faster drying for large volumes of wood, particularly in solar kilns, the most common hybridization is done with commercial paraffin wax. The PCM is chosen on the basis of the dryer operating temperature. The PCM-integrated dryer's efficiency can be further increased using an electrical heat exchanger [42]. Khouya and Draoui [43] carried out research in a hybrid kiln using several PCMs. According to the findings, the thermal storage unit's mode of operation, board thickness, mass flow rate, and recycling heat process all have an impact on drying time. Additionally, compared to a drying technique without recovered heat, adopting an air recycling process reduced the amount of energy provided to the system and the drying time by approximately 47%. The present study also reveals that by using PCM, the average thermal efficiency increased from 19.75% to 23.85%, which might be further increased using electrical-heat exchanger. The high average thermal energy efficiency in (with PCM) scenario supports utilizing coconut oil as thermal energy storage material. The cost of heating 1 kg of hot air is an important criterion for an economically sustainable dryer wiith 7 Hrs/Day operational hybrid PCM dryer, it was evaluated as 0.0074 US dollars [44], in the present study, this value is 0.0058 EUR. EPBT for greenhouse dryers was 1.14 years, and CO2 emission per year is 17.6 kg per year for drying tomato flakes[45] as compared to 1.13 years releasing 64.09 kgs of CO2 per year in the present study. However, the next investigations will attempt large-volume experiments and CFD simulations to better understand the associated physical parameters.

Table 5. Solar drying of distinct wood fuels under different drying conditions.

Solar Dryer	Wood Fuel	PCM	Drying Time (h)	Temperature range (°C)	Intial and final moisture content	Average energy efficiency (%)	Ref.
Solar greenhouse dryer	Woodchips	-	19	30.7-55.9	50-10 (%)	-	[41]
Solar-electrical dryer	Redpine wood stacks	Commercial PCM RT55	168	40-90	0.8-0.1 (kg_{wb}/kg_{db})	79	[42]
Solar Kiln with PCM	Red pine, Spruce and Beech wood	RT64 (Paraffin), RT82 (Paraffin) and Erythritol (Alcoholic sugar)	600	47-94	0.5-0.1 (kg_{wb}/kg_{db})	47	[43]
Solar Kiln with PCM	Wood stacks	Paraffin wax	07	30-70	70-6 (%)	-	[46]
Present study (without PCM)	Woodchips Pellets Sawdust	-	22	18-70	45-16 (%) 37-12 (%) 39-10 (%)	19.75	
Present study (with PCM)	Woodchips Pellets Sawdust	Coconut oil	22	18-70	45-11 (%) 37-08 (%) 39-06 (%)	23.85	

5. NEW SCIENTIFIC RESULTS – THESIS

T1- The forced convection solar cabinet dryer, operating under standard solar radiation conditions, showcases a remarkable temperature differential of 10–20°C between its inlet and outlet. During peak solar hours, the system attains a noteworthy maximum temperature of 60°C. The overall system efficiency of the dryer with respect to the woodchips, sawdust, and wood pellets was found to be (19.04–29.9)%, (23.34–33.2)%, and (21.11–31.1)%. Intriguingly, the observed superior drying rates of sawdust and pellets in comparison to woodchips underscore the material-specific performance enhancements achievable through the optimized solar drying systems.

T2- The investigation of cabinet type dryer elucidates the application of Artificial Neural Network (ANN) modeling, implemented in the NN (Neural network) tool of MATLAB software, for the validation and prediction of final moisture content in solar drying processes. The model, featuring a single hidden layer optimized under Levenberg-Marquardt, was meticulously trained using a random dataset derived from experimental trials, spanning 10,000 iterations. Employing tan-sigmoid activation function for hidden neurons for linear output neurons, the model achieved notable validation performance, registering a minimal mean square error of 2.4949 at epoch 993. The coefficient of correlation (R), a pivotal metric indicating model robustness, demonstrated exceptional goodness-of-fit with values of 1, 0.995, 0.970, and 0.990 for training, validation, test, and overall datasets, respectively. This achievement signifies the model's efficacy in accurately validating final moisture content for solar drying processes.

T3- The hybrid dryer, integrating coconut oil as a Phase Change Material (PCM) for energy storage and operating under constant artificial solar radiation, achieved a maximum temperature of 70°C, surpassing the capabilities of the standalone forced convection solar cabinet dryer. Notably, the hybrid system exhibits extended retention of useful heat for 3 hours post-radiation switch-off, showcasing its ability to mitigate intermittent irradiation challenges. The analysis of exergy efficiencies reveals a notable performance range between 13.1% and 14.8%, highlighting the system's effectiveness in harnessing and utilizing energy resources. The thermal energy efficiency during the four hours of heat retention in the case of PCM increases by 63.64%.

T4- The solar drying of wood fuels emerges as a sustainable solution, showcasing substantial reductions in energy losses and CO2 emissions. The integration of a hybrid dryer with Phase

Change Material (PCM) further enhances these environmental benefits. In the hybrid dryer with PCM, wood fuels exhibit remarkable final moisture content levels, measured at 11% for wood chips, 8% for pellets, and 6% for sawdust. Economic assessments predict a commendable lifespan of approximately five years, with a calculated cost of 0.0058 EUR per kg of drying air. Moreover, this sustainable approach results in an annual emission of 64.09 kgs of CO_2, underscoring the environmental and economic viability of solar drying systems for wood fuels. This finding contributes to the understanding of the multifaceted advantages offered by solar drying in promoting green and economically feasible wood fuel drying solutions.

T5- A comprehensive analysis of solar energy infrastructure in Hungary uncovers concentrated solar parks boasting nearly 10 MW capacity, predominantly located in the northeastern region. This investigation, spanning the years from 2010 to 2020, identifies untapped solar potential in the southern and eastern areas of the country. The observed yearly photovoltaic (PV) production in these regions ranges between 1100 and 1250 KWh, complemented by an annual plane radiation value in the span of 1400–1600 KWh/m² and can be instrumental in developing PV-based hybrid solar dryers. Notably, the minimal overall variation in these metrics signifies the consistent and promising solar energy potential in the untapped eastern and southern regions of Hungary.

LIST OF PUBLICATIONS RELATED TO THE TOPIC OF THE RESEARCH FIELD

[S1] Kumar, Baibhaw, Gábor Szepesi, Zoltán Szamosi, and Gyula Kramer. Analysis of a Combined Solar Drying System for Wood-Chips, Sawdust, and Pellets. Sustainability.15 (3):1791. (2023) MTMT: 33582995 https://doi.org/10.3390/su15031791 Q2(IF: 3.8 (2023))

[S2] Kumar, Baibhaw, Raj K, Arun, Gábor Szepesi and Zoltán Szamosi. A conspectus review on solar drying of wood: regional and technical contrivances. Journal of Thermal Analysis Calorimatery. (1-25) (2023). MTMT: 33721596 https://doi.org/10.1007/s10973-023-12093-5 Q2 (IF: 4.75) (2023)

[S3] Kumar, Baibhaw, Gábor Szepesi and Zoltán Szamosi. Optimisation techniques for solar drying systems: a review on modelling, simulation, and financial assessment approaches, International Journal of Sustainable Energy, 42:1, 182-208, (2023) MTMT: 33714404 DOI: 10.1080/14786451.2023.2185870 Q2 (IF: 3.1 (2022))

[S4] Kumar, Baibhaw, Gábor Szepesi, Zsolt Čonka, Michal Kolcun, Zsolt Péter, László Berényi, and Zoltán Szamosi. Trendline Assessment of Solar Energy Potential in Hungary and Current Scenario of Renewable Energy in the Visegrád Countries for Future Sustainability, Sustainability, Vol.13, issue 10, P 5462, (2021) MTMT: 32017468 https://doi.org/10.3390/su13105462 Q2 (IF: 3.8) (2021)

[S5] Kumar, Baibhaw, Gábor Szepesi and Zoltán Szamosi. Drying behaviour observations for wood chips of grade EN 14961, Multidiszciplináris tudományok: a Miskolc egyetem közleménye 11: 4 pp.151-156.,6p. (2021) MTMT: 31937254 https://doi.org/10.35925/j.multi.2021.4.19

[S6] Kumar, Baibhaw, Gábor Szepesi and Zoltán Szamosi. Design and development of natural convective solar dryer, Multidiszciplináris tudományok: a Miskolc egyetem közleménye 11: 4 pp.144-150., 7p. (2021) MTMT: 31931131 https://doi.org/10.35925/j.multi.2021.4.18

[S7] Kumar, Baibhaw, László Berényi, Gábor Szepesi and Zoltán Szamosi. Business model analysis for the scope of entrepreneurship in a solar drying field in the European region. ENTREPRENEURSHIP IN THE RAW MATERIALS SECTOR, 85. (2022). MTMT:32740220 http://dx.doi.org/10.1201/9781003259954-9

REFERENCES

[1] G. Lianbai, "Recent Research and Development in Wood Drying Technologies in China," *Drying Technology*, vol. 25, no. 3, pp. 463–469, Mar. 2007, doi: 10.1080/07373930601183900.

[2] P. Singh, V. Shrivastava, and A. Kumar, "Recent developments in greenhouse solar drying: A review," *Renewable and Sustainable Energy Reviews*, vol. 82, pp. 3250–3262, 2018, doi: https://doi.org/10.1016/j.rser.2017.10.020.

[3] B. Dundar, R. G. McGarvey, and F. X. Aguilar, "Optimal multi-state partnerships for woody biomass co-firing incorporating a demand-response function for biomass procurement," *Optim Lett*, vol. 16, no. 3, pp. 821–844, 2022, doi: 10.1007/s11590-021-01747-8.

[4] J. Yi, X. Li, J. He, and X. Duan, "Drying efficiency and product quality of biomass drying: a review," *Drying Technology*, vol. 38, no. 15, pp. 2039–2054, Nov. 2020, doi: 10.1080/07373937.2019.1628772.

[5] B. Lamrani, N. Bekkioui, M. Simo-Tagne, and M. C. Ndukwu, "Recent progress in solar wood drying: An updated review," *Drying Technology*, vol. 41, no. 5, pp. 605–627, Apr. 2023, doi: 10.1080/07373937.2022.2112048.

[6] L. Blanco-Cano, A. Soria-Verdugo, L. M. Garcia-Gutierrez, and U. Ruiz-Rivas, "Evaluation of the Maximum Evaporation Rate in Small-Scale Indirect Solar Dryers," *Journal of Solar Energy Engineering, Transactions of the ASME*, vol. 138, no. 2, pp. 1–4, 2016, doi: 10.1115/1.4032351.

[7] O. A. Babar, A. Tarafdar, S. Malakar, V. K. Arora, and P. K. Nema, "Design and performance evaluation of a passive flat plate collector solar dryer for agricultural products," *J Food Process Eng*, vol. 43, no. 10, 2020, doi: 10.1111/jfpe.13484.

[8] O. J. Alamu, C. N. Nwaokocha, and O. Adunola, "Design and Construction of a Domestic Passive Solar Food Dryer," *Leonardo Journal of Sciences*, no. 16, pp. 71–82, 2010.

[9] H. E. Ã, "Experimental energy and exergy analysis of a double-flow solar air heater having different obstacles on absorber plates," vol. 43, pp. 1046–1054, 2008, doi: 10.1016/j.buildenv.2007.02.016.

[10] Ã. Kurtbas and A. Durmus, "Efficiency and exergy analysis of a new solar air heater," vol. 29, pp. 1489–1501, 2004, doi: 10.1016/j.renene.2004.01.006.

[11] G. Habtay, M. A. Al-Neama, J. Buzas, and I. Farkas, "Experimental Performance of Solar Air Heaters for Drying Applications," *European Journal of Energy Research*, vol. 1, no. 5, pp. 4–10, 2021, doi: 10.24018/ejenergy.2021.1.5.29.

[12] S. Hatami, G. Payganeh, and A. Mehrpanahi, "Energy and exergy analysis of an indirect solar dryer based on a dynamic model," *J Clean Prod*, vol. 244, p. 118809, 2020, doi: https://doi.org/10.1016/j.jclepro.2019.118809.

[13] D. Bahrehmand, M. Ameri, and M. Gholampour, "Energy and exergy analysis of different solar air collector systems with forced convection," *Renew Energy*, vol. 83, pp. 1119–1130, 2015, doi: https://doi.org/10.1016/j.renene.2015.03.009.

[14] T. Kh. Abdelkader, Q. Fan, E. S. Gaballah, S. Wang, and Y. Zhang, "Energy and Exergy Analysis of a Flat-Plate Solar Air Heater Artificially Roughened and Coated with a Novel Solar Selective Coating," *Energies*, vol. 13, no. 4. 2020. doi: 10.3390/en13040997.

[15] H. Krabch, R. Tadili, and A. Idrissi, "Design, realization and comparison of three passive solar dryers. Orange drying application for the Rabat site (Morocco)," *Results in Engineering*, vol. 15, p. 100532, 2022, doi: https://doi.org/10.1016/j.rineng.2022.100532.

[16] V. Rasooli Sharabiani, M. Kaveh, R. Abdi, M. Szymanek, and W. Tanaś, "Estimation of moisture ratio for apple drying by convective and microwave methods using artificial neural network modeling," *Sci Rep*, vol. 11, no. 1, p. 9155, 2021, doi: 10.1038/s41598-021-88270-z.

[17] A. K. Kushwah, M. K. G. Gaur, A. K. Kumar, and P. S. Singh, "Application of ANN and prediction of drying behavior of mushroom drying in side hybrid greenhouse solar dryer : An experimental validation," vol. 8, no. 2, 2022, doi: 10.18186/thermal.1086189.

[18] A. Sadadou, S. Hanini, M. Laidi, and A. Rezrazi, "ANN-based Approach to Model MC / DR of Some Fruits Under Solar Drying," vol. 70, pp. 233–242, 2021.

[19] A. H. Elsheikh, S. W. Sharshir, M. Abd Elaziz, A. E. Kabeel, W. Guilan, and Z. Haiou, "Modeling of solar energy systems using artificial neural network: A comprehensive review," *Solar Energy*, vol. 180, pp. 622–639, 2019, doi: https://doi.org/10.1016/j.solener.2019.01.037.

[20] B. K. Bala, M. A. Ashraf, M. A. Uddin, and S. Janjai, "Experimental and neural network prediction of the performance of a solar tunnel drier for drying jackfruit bulbs and leather," *J Food Process Eng*, vol. 28, no. 6, pp. 552–566, 2005, doi: 10.1111/j.1745-4530.2005.00042.x.

[21] S. Tiwari, "ANN and mathematical modelling for moisture evaporation with thermal modelling of bitter gourd flakes drying in SPVT solar dryer," *Heat and Mass Transfer*, vol. 56, no. 10, pp. 2831–2845, 2020, doi: 10.1007/s00231-020-02886-x.

[22] J. F. Hinojosa, S. F. Moreno, and V. M. Maytorena, "Low-Temperature Applications of Phase Change Materials for Energy Storage: A Descriptive Review," *Energies*, vol. 16, no. 7. 2023. doi: 10.3390/en16073078.

[23] S. Hasbi, K. Y. Leong, K. Z. K. Ahmad, A. R. Norwazan, and M. S. Saharudin, "Development of Coconut Oil/Capric Acid Eutectic Phase Change Material with Graphene as Latent Thermal Energy Storage," *International Journal of Automotive and Mechanical Engineering*, vol. 20, no. 1, pp. 10247–10257, 2023, doi: 10.15282/ijame.20.1.2023.07.0792.

[24] L. Safira, N. Putra, T. Trisnadewi, E. Kusrini, and T. M. I. Mahlia, "Thermal properties of sonicated graphene in coconut oil as a phase change material for energy storage in building applications," *International Journal of Low-Carbon Technologies*, vol. 15, no. 4, pp. 629–636, 2020, doi: 10.1093/ijlct/ctaa018.

[25] C. A. Saleel, "A review on the use of coconut oil as an organic phase change material with its melting process, heat transfer, and energy storage characteristics," *J Therm Anal Calorim*, vol. 147, no. 7, pp. 4451–4472, 2022, doi: 10.1007/s10973-021-10839-7.

[26] C. A. Saleel, M. A. Mujeebu, and S. Algarni, "Coconut oil as phase change material to maintain thermal comfort in passenger vehicles: An experimental analysis," *J Therm Anal Calorim*, vol. 136, no. 2, pp. 629–636, 2019, doi: 10.1007/s10973-018-7676-y.

[27] A. Afzal *et al.*, "Human thermal comfort in passenger vehicles using an organic phase change material– an experimental investigation, neural network modelling, and optimization," *Build Environ*, vol. 180, p. 107012, 2020, doi: https://doi.org/10.1016/j.buildenv.2020.107012.

[28] D. M. Martínez, B. W. Ebenhack, and T. P. Wagner, "Chapter 1 - Introductory concepts," D. M. Martínez, B. W. Ebenhack, and T. P. B. T.-E. E. Wagner, Eds., Elsevier, 2019, pp. 1–33. doi: https://doi.org/10.1016/B978-0-12-812111-5.00001-9.

[29] B. Europe, "World Pellet Map." Accessed: Jul. 25, 2022. [Online]. Available: https://epc.bioenergyeurope.org/about-pellets/pellets-statistics/world-pellet-map/

[30] D. Almeida and E. Marques, "Solar Drying Acacia- Influence in Pellets Quality :," in *22nd International Congress of Mechanical Engineering (COBEM 2013)*, 2013, pp. 6742–6752.

[31] M. N. A. Hawlader, M. S. Uddin, and M. M. Khin, "Microencapsulated PCM thermal-energy storage system," *Appl Energy*, vol. 74, no. 1, pp. 195–202, 2003, doi: https://doi.org/10.1016/S0306-2619(02)00146-0.

[32] A. K. Raj, M. Srinivas, and S. Jayaraj, "A cost-effective method to improve the performance of solar air heaters using discrete macro-encapsulated PCM capsules for drying applications," *Appl Therm Eng*, vol. 146, pp. 910–920, 2019, doi: https://doi.org/10.1016/j.applthermaleng.2018.10.055.

[33] G. Tsatsaronis, "Definitions and nomenclature in exergy analysis and exergoeconomics," *Energy*, vol. 32, no. 4, pp. 249–253, 2007, doi: https://doi.org/10.1016/j.energy.2006.07.002.

[34] B. Kumar, L. G. Szepesi, and Z. Szamosi, "Drying behaviour observations for wood chips of grade EN14961," *Multidiszciplináris tudományok*, vol. 11, no. 4, pp. 151–156, 2021, doi: 10.35925/j.multi.2021.4.19.

[35] K. Baibhaw, G. L. Szepesi, and Z. Szamosi, "Design and Development of natural convective solar dryer," *Multidisciplinary Sciences*, vol. 11, no. 4, pp. 144–150, 2021, doi: https://doi.org/10.35925/j.multi.2021.4.18.

[36] B. Kumar, G. Szepesi, Z. Szamosi, and G. Krámer, "Analysis of a Combined Solar Drying System for Wood-Chips, Sawdust, and Pellets," *Sustainability*, vol. 15, no. 3. 2023. doi: 10.3390/su15031791.

[37] G. Pintér, H. Zsiborács, N. H. Baranyai, A. Vincze, and Z. Birkner, "The economic and geographical aspects of the status of small-scale photovoltaic systems in hungary-a case study," *Energies (Basel)*, vol. 13, no. 13, 2020, doi: 10.3390/en13133489.

[38] G. A. Vokas, G. C. Zoridis, and K. V. Lagogiannis, "Single and Dual Axis PV Energy Production over Greece: Comparison between Measured and Predicted Data," *Energy Procedia*, vol. 74, pp. 1490–1498, 2015, doi: 10.1016/j.egypro.2015.07.798.

[39] S. Park, Y. Kim, N. J. Ferrier, S. M. Collis, R. Sankaran, and P. H. Beckman, "Prediction of Solar Irradiance and Photovoltaic Solar Energy Product Based on Cloud Coverage Estimation Using Machine Learning Methods," *Atmosphere (Basel)*, vol. 12, no. 3, p. 395, 2021, doi: 10.3390/atmos12030395.

[40] European Commission, "PHOTOVOLTAIC GEOGRAPHICAL INFORMATION SYSTEM." [Online]. Available: https://re.jrc.ec.europa.eu/pvg_tools/en/

[41] A.-J. Perea-Moreno, A. Juaidi, and F. Manzano-Agugliaro, "Solar greenhouse dryer system for wood chips improvement as biofuel," *J Clean Prod*, vol. 135, pp. 1233–1241, 2016, doi: https://doi.org/10.1016/j.jclepro.2016.07.036.

[42] B. Lamrani and A. Draoui, "Modelling and simulation of a hybrid solar-electrical dryer of wood integrated with latent heat thermal energy storage system," *Thermal Science and Engineering Progress*, vol. 18, p. 100545, 2020, doi: https://doi.org/10.1016/j.tsep.2020.100545.

[43] A. Khouya and A. Draoui, "Computational drying model for solar kiln with latent heat energy storage: Case studies of thermal application," *Renew Energy*, vol. 130, pp. 796–813, 2019, doi: 10.1016/j.renene.2018.06.090.

[44] A. K. Raj, M. Srinivas, and S. Jayaraj, "A cost-e ff ective method to improve the performance of solar air heaters using discrete macro-encapsulated PCM capsules for drying applications," *Appl Therm Eng*, vol. 146, no. June 2018, pp. 910–920, 2019, doi: 10.1016/j.applthermaleng.2018.10.055.

[45] O. Prakash and A. Kumar, "Environomical analysis and mathematical modelling for tomato flakes drying in a modified greenhouse dryer under active mode," *International Journal of Food Engineering*, vol. 10, no. 4, pp. 669–681, 2014, doi: 10.1515/ijfe-2013-0063.

[46] S. Kumar and V. S. Kishankumar, "Thermal energy storage for a solar wood drying kiln: estimation of energy requirement," *Journal of the Indian Academy of Wood Science*, vol. 13, no. 1, pp. 33–37, 2016, doi: 10.1007/s13196-016-0162-x.